

1 **Urban organic aerosol composition in Eastern China differs from North to South: Molecular**
2 **insight from a liquid chromatography-Orbitrap mass spectrometry study**

3 Kai Wang^{1,2,4}, Ru-Jin Huang¹, Martin Brüggemann³, Yun Zhang², Lu Yang¹, Haiyan Ni¹, Jie Guo¹,
4 Meng Wang¹, Jiajun Han⁵, Merete Bilde⁴, Marianne Glasius⁴, and Thorsten Hoffmann²

5 ¹State Key Laboratory of Loess and Quaternary Geology (SKLLQG), Center for Excellence in
6 Quaternary Science and Global Change, and Key Laboratory of Aerosol Chemistry and Physics,
7 Institute of Earth and Environment, Chinese Academy of Sciences, Xi'an 710061, China

8 ²Institute of Inorganic and Analytical Chemistry, Johannes Gutenberg University Mainz,
9 Duesbergweg 10–14, Mainz 55128, Germany

10 ³Atmospheric Chemistry Department (ACD), Leibniz Institute for Tropospheric Research
11 (TROPOS), Permoserstraße 15, 04318 Leipzig, Germany

12 ⁴Department of Chemistry, Aarhus University, Langelandsgade 140, DK-8000 Aarhus C, Denmark

13 ⁵Department of Chemistry, University of Toronto, 80 St. George Street, M5S3H6 Toronto, Canada

14 Corresponding Author: Ru-Jin Huang (rujin.huang@ieecas.cn) and Thorsten Hoffmann
15 (t.hoffmann@uni-mainz.de)

16

17

18

19

20

21

22

23

24

25

26

27 **Abstract:**

28 Air pollution by particulate matter in China affects human health, the ecosystem and the climate.
29 However, the chemical composition of particulate aerosol, especially of the organic fraction, is still
30 not well understood. In this study, particulate aerosol samples with a diameter of $\leq 2.5 \mu\text{m}$ ($\text{PM}_{2.5}$)
31 were collected in January 2014 in three cities located in Northeast, East and Southeast China,
32 namely Changchun, Shanghai and Guangzhou. Organic aerosol (OA) in the $\text{PM}_{2.5}$ samples was
33 analyzed by ultrahigh performance liquid chromatography (UHPLC) coupled to high-resolution
34 Orbitrap mass spectrometry in both negative mode (ESI⁻) and positive mode electrospray
35 ionization (ESI⁺). After non-target screening including the assignment of molecular formulas, the
36 compounds were classified into five groups based on their elemental composition, i.e., CHO,
37 CHON, CHN, CHOS and CHONS. The CHO, CHON and CHN groups present the dominant signal
38 abundances of 81–99.7% in the mass spectra and the majority of these compounds were assigned
39 to mono- and polyaromatics, suggesting that anthropogenic emissions are a major source of urban
40 OA in all three cities. However, the chemical characteristics of these compounds varied between
41 the different cities. The degree of aromaticity and the number of polyaromatic compounds were
42 substantially higher in samples from Changchun, which could be attributed to the large emissions
43 from residential heating (i.e. coal combustion) during winter time in Northeast China. Moreover,
44 the ESI⁻ analysis showed higher H/C and O/C ratios for organic compounds in Shanghai and
45 Guangzhou compared to samples from Changchun, indicating that OA undergoes more intense
46 photochemical oxidation processes in lower latitude regions of China and/or is affected to a larger
47 degree by biogenic sources. The majority of sulfur-containing compounds (CHOS and CHONS) in
48 all cities were assigned to aliphatic compounds with low degrees of unsaturation and aromaticity.
49 Here again, samples from Shanghai and Guangzhou show a greater chemical similarity but differ
50 largely from those from Changchun. It should be noted that the conclusions drawn in this study are
51 mainly based on comparison of molecular formulas weighted by peak abundance, and thus, are
52 associated with inherent uncertainties due to different ionization efficiencies for different organic
53 species.

54 **1. Introduction**

55 In the last decades, China has experienced rapid industrialization and urbanization accompanied by
56 severe and persistent particulate air pollution (Huang et al., 2014; Sun et al., 2014; Ding et al., 2016;
57 Song et al., 2018; Shi et al., 2019; Xu et al., 2019). These particulate air pollution extremes can not
58 only influence the regional air quality and human health in China, but also lead to a global

59 environmental problem due to long-distance transport of pollutants. To better understand the effects
60 of air pollution on air quality and human health, chemical characterization of fine particle
61 (particulate matter with an aerodynamic diameter of less than 2.5 μm , or $\text{PM}_{2.5}$) is crucial. However,
62 the chemical composition of $\text{PM}_{2.5}$ in China is still poorly understood due to a wide variety of
63 natural and anthropogenic sources as well as complex multiphase chemical reactions (Lin et al.,
64 2012a; Huang et al., 2014; Ding et al., 2016; Wang et al., 2017; Wang et al., 2018; An et al., 2019;
65 Tong et al., 2019; Wang et al., 2019a; Wang et al., 2019b). In particular, compared to the fairly
66 well understood nature of the inorganic fraction of aerosol, the organic fraction, also named organic
67 aerosol (OA), is considerably less understood in terms of chemical composition, corresponding
68 precursors, sources and formation mechanisms (Huang et al., 2017).

69 During pollution events in China, OA accounts for as high as more than 50% of the total mass of
70 fine particle (An et al., 2019). Chemical compounds in OA cover a large complexity of species
71 including alcohols, aldehydes, carboxylic acids, imidazoles, organosulfates, organonitrates and
72 polycyclic aromatic hydrocarbons (PAHs) (Lin et al., 2012a; Rincón et al., 2012; Kourtchev et al.,
73 2014; Wang et al., 2018; Elzein et al., 2019; Wang et al., 2019a). Thus, the capacity of traditional
74 analytical techniques is limited to identify the compounds in OA and the majority (> 70%) of OA
75 has not been identified yet as specific compounds (Hoffmann et al., 2011). The insufficient
76 knowledge of chemical composition of OA hinders a better understanding of the sources, formation
77 and atmospheric processes of air pollution in China.

78 Recently, ultrahigh resolution mass spectrometry (UHRMS), such as Fourier transform ion
79 cyclotron resonance mass spectrometry (FTICR-MS) and Orbitrap-MS, coupled with soft
80 ionization sources (e.g., electrospray ionization (ESI) and atmospheric pressure chemical ionization
81 (APCI)) have been introduced to elucidate the molecular composition of OA (Nizkorodov et al.,
82 2011; Lin et al., 2012a; Lin et al., 2012b; Rincón et al., 2012; Noziere et al., 2015; Kourtchev et al.,
83 2016; Tong et al., 2016; Tu et al., 2016; Brüggemann et al., 2017; Wang et al., 2017; Fleming et
84 al., 2018; Laskin et al., 2018; Song et al., 2018; Wang et al., 2018; Brüggemann et al., 2019;
85 Daellenbach et al., 2019; Ning et al., 2019; Wang et al., 2019a). Due to the two outstanding features
86 of high resolving power and high mass accuracy, UHRMS can give precise elemental compositions
87 of individual organic compounds. However, UHRMS studies on Chinese urban OA are very limited.
88 Wang et al. (Wang et al., 2017) characterized OA in Shanghai and showed variations in chemical
89 composition among different months and between daytime and nighttime. Our recent Orbitrap MS
90 study (Wang et al., 2018) showed that wintertime OA in $\text{PM}_{2.5}$ collected in Beijing, China and
91 Mainz, Germany were very different in terms of chemical composition. In contrast, for summertime

92 OA from Germany and China, Brüggemann et al. (2019) found similar compounds and
93 concentrations of terpenoid organosulfates in PM₁₀, demonstrating that biogenic emission can
94 significantly affect OA composition at both locations. Ning et al. (2019) analyzed the OA collected
95 in a coastal Chinese city (Dalian) and found that more organic compounds were identified in haze
96 days compared to non-haze days. Nonetheless, since severe particulate pollution in China occurs
97 on a large-scale, more UHRMS studies are needed to fully elucidate the chemical composition of
98 OA in different Chinese cities.

99 In this study, PM_{2.5} aerosol samples were collected in three Chinese cities, i.e., Changchun,
100 Shanghai and Guangzhou, and their organic fraction was analyzed using ultra-high-performance
101 liquid chromatography (UHPLC) coupled with Orbitrap-MS. The Chinese cities of Changchun,
102 Shanghai and Guangzhou are located in the Northeast, East and Southeast of China, which are
103 major populated regions in China with a population of 7.5, 24 and 15 million, respectively. The
104 geographic locations of these three cities cover a large latitude spanning from 23.12°N to 43.53°N
105 resulting in different meteorological conditions, including intensity and duration of sunlight,
106 average daily temperature and monsoon climate. In addition, the industrial structure, energy
107 consumption and energy sources in these three cities are different, such as much more heavy
108 industries (e.g., coal chemical industry and steelworks) in Northeast China (Zhang, 2008), which
109 can cause difference in anthropogenic emissions, and can therefore influence the chemical
110 composition of urban OA. Moreover, OA is strongly affected by residential coal combustion during
111 winter in Northeast China (Huang et al., 2014; An et al., 2019). Therefore, this study presents a
112 comprehensive overview of chemical composition of OA in three representative Chinese cities
113 during pollution episodes, which eventually can improve our understanding of OA effects on
114 climate and public health and also provide a chemical database for haze mitigation strategies in
115 China.

116 **2. Experimental**

117 **2.1 PM_{2.5} samples**

118 Three 24-h integrated urban PM_{2.5} samples were collected during severe haze pollution events with
119 daily average PM_{2.5} mass concentration higher than 115 µg m⁻³ in each of the three Chinese cities:
120 Changchun (43.54° N, 125.13° E, 1.5 m above the ground), Shanghai (31.30° N, 121.50° E, 20 m
121 above the ground) and Guangzhou (23.07° N, 113.21° E, 53 m above the ground), which are located
122 in the Northeast, East and Southeast regions of China, respectively (see Fig. 1). Samples in
123 Changchun were collected on 4, 24 and 29 of January 2014 with PM_{2.5} mass concentrations of

124 185–222 $\mu\text{g m}^{-3}$, samples in Shanghai were collected on 1, 19 and 20 of January 2014 with $\text{PM}_{2.5}$
125 mass concentrations of 159–172 $\mu\text{g m}^{-3}$ and samples in Guangzhou were collected on 5, 6 and 11
126 of January 2014 with $\text{PM}_{2.5}$ mass concentrations of 138–152 $\mu\text{g m}^{-3}$. Further details (e.g., the daily
127 average concentrations of $\text{PM}_{2.5}$, SO_2 , NO_2 , CO and O_3 , the average temperature and the daily solar
128 radiation value during sampling dates) are presented in Table S1, the 48 hours back trajectories of
129 air arriving at the three sampling sites during the sampling periods are shown in Fig. S1. All $\text{PM}_{2.5}$
130 samples were collected on prebaked quartz-fiber filters (20.3×25.4 cm) using a high-volume $\text{PM}_{2.5}$
131 sampler at a flow rate of 1.05 $\text{m}^3 \text{min}^{-1}$ (Tisch Environmental, USA) and at each sampling site field
132 blanks were taken. After sample collection, filters were stored at $-20\text{ }^\circ\text{C}$ until analysis.

133 **2.2 Sample analysis**

134 Detailed description on the filter sample extraction and UHPLC–Orbitrap MS analysis can be found
135 in our previous studies (Wang et al., 2018; Wang et al., 2019a). Briefly, a part of the filters (around
136 1.13 cm^2 , corresponding to about 600 μg particle mass in each extracted filter) was extracted three
137 times with 1.0–1.5 mL of acetonitrile-water (8/2, v/v) in an ultrasonic bath. The extracts were
138 combined, filtered through a 0.2 μm Teflon syringe filter and evaporated to almost dryness under
139 a gentle nitrogen stream. Finally, the residue was redissolved in 1000 μL acetonitrile-water (1/9,
140 v/v) to reach the total particulate mass concentration of around 600 $\mu\text{g mL}^{-1}$ for the following
141 analysis.

142 Compared to the direct infusion method applied in other UHRMS studies (Lin et al., 2012a; Lin et
143 al., 2012b; Rincón et al., 2012; Kourtchev et al., 2016; Fleming et al., 2018), the UHPLC technique
144 was used in this study, which could separate and concentrate the compounds before they entered
145 the ion source, reducing the ionization suppression and increasing the sensitive of the measurement.
146 In addition, it can provide separation of some compounds and information of retention time of the
147 compounds, which is useful for the identification of the compounds and the separation of isomers.
148 The analytes were separated using a Hypersil Gold column (C18, 50 x 2.0 mm, 1.9 μm particle size)
149 with mobile phases consisting of (A) 0.04% formic acid and 2% acetonitrile in MilliQ water and
150 (B) 2% water in acetonitrile. Gradient elution was applied with the A and B mixture at a flow rate
151 of 500 $\mu\text{L min}^{-1}$ as follows: 0–1.5 min 2% B, 1.5–2.5 min from 2% to 20% B (linear), 2.5–5.5 min
152 20% B, 5.5–6.5 min from 20% to 30% B (linear), 6.5–7.5 min from 30% to 50% B (linear), 7.5–8.5
153 min from 50% to 98% B (linear), 8.5–11.0 min 98% B, 11.0–11.05 min from 98% to 2% B (linear),
154 and 11.05–11.1 min 2% B. The Q Exactive Hybrid Quadrupole-Orbitrap MS was equipped with a
155 heated ESI source at 120 $^\circ\text{C}$, applying a spray voltage of -3.3 kV and 4.0 kV for negative ESI mode

156 (ESI⁻) and positive ESI mode (ESI⁺), respectively. The mass scanning range was set from m/z 50
157 to 500 with a resolving power of 70,000 @ m/z 200. The Orbitrap MS was externally calibrated
158 before each measurement sequence using an Ultramark 1621 solution (Sigma–Aldrich, Germany)
159 providing mass accuracy of the instrument lower than 3 ppm. Each sample was measured in
160 triplicate with an injection volume of 10 μ L.

161 **2.3 Data processing**

162 A non-target peak picking software (SIEVE[®], Thermo Fisher Scientific, Germany) was used to find
163 significant peaks in the LC-MS dataset and to calculate all mathematically possible chemical
164 formulas for ions signals with a sample-to-blank abundance ratio ≥ 10 using a mass tolerance of \pm
165 2 ppm. The permitted maximum elemental number of atoms was set as follows: ¹²C (39), ¹H (72),
166 ¹⁶O (20), ¹⁴N (7), ³²S (4), ³⁵Cl (2) and ²³Na (1) (Kind and Fiehn, 2007; Lin et al., 2012a; Wang et
167 al., 2018). To remove the chemically unreasonable formulas, further constraint was applied by
168 setting H/C, O/C, N/C, S/C and Cl/C ratios in the ranges of 0.3–3, 0–3, 0–1.3, 0–0.8 and 0–0.8
169 (Kind and Fiehn, 2007; Lin et al., 2012a; Rincón et al., 2012; Wang et al., 2018; Zielinski et al.,
170 2018), respectively. For chemical formula C_cH_hO_oN_nS_sCl_x, the double bond equivalent (DBE) was
171 calculated by the equation: $DBE = (2c + 2 - h - x + n) / 2$. The aromaticity equivalent (X_C) as a
172 modified index for aromatic compounds was obtained using the equation: $X_C = [3(DBE - (p \times o +$
173 $q \times n)) - 2] / [DBE - (p \times o + q \times n)]$, where p and q, respectively, refer to the fraction of oxygen
174 and sulfur atoms involved in the π -bond structure of a compound. As such the values of p and q
175 vary between compound categories (Yassine et al., 2014). For example, carboxylic acids and esters
176 are characterized using p = q = 0.5, while p = q = 1 and p = q = 0 are used for carbonyl and hydroxyl,
177 respectively. Since it is impossible to identify the structures of the hundreds of formulas observed
178 in this study, we cannot know the exact values of p and q in an individual compound. Therefore, in
179 this study, p = q = 0.5 was applied for compounds detected in ESI⁻ as carboxylic compounds are
180 preferably ionized in negative mode. However, because of the high complexity of the mass spectra
181 in ESI⁺, p = q = 1 was used in ESI⁺ to avoid an overestimation of the amount of aromatics.
182 Moreover, for $DBE \leq (p \times o + q \times n)$ or $X_C \leq 0$, X_C was defined as zero. Furthermore, in ESI⁻, for
183 odd numbers of (p \times o + q \times n), the value of (p \times o + q \times n) was rounded down to the lower integer.
184 $X_C \geq 2.50$ and $X_C \geq 2.71$ have been suggested as unambiguous minimum criteria for the presence
185 of monoaromatics and polyaromatics, respectively (Yassine et al., 2014).

186 Comparing the peak abundance has been used in recent UHRMS studies (Wang et al., 2017;
187 Fleming et al., 2018; Song et al., 2018; Ning et al., 2019) to illustrate the relative importance of

188 specific types of compounds. However, it should be noted that different organic compounds have
189 different signal response in the mass spectrometer due to the differences in ionization and
190 transmission efficiencies (Schmidt et al., 2006; Leito et al., 2008; Perry et al., 2008; Krueve et al.,
191 2014). Therefore, uncertainties may exist when comparing the peak areas among compounds. In
192 this work, we assume that all organic compounds have the same peak abundance response in the
193 mass spectrometer. The peak abundance-weighted average molecular mass (MM), elemental ratios,
194 DBE, and Xc for formula $C_cH_hO_oN_nS_sCl_x$ were calculated using following equations:

$$195 \text{MM}_{\text{avg}} = \sum (\text{MM}_i \times A_i) / \sum A_i$$

$$196 \text{O/C}_{\text{avg}} = \sum (\text{O/C}_i \times A_i) / \sum A_i$$

$$197 \text{H/C}_{\text{avg}} = \sum (\text{H/C}_i \times A_i) / \sum A_i$$

$$198 \text{DBE}_{\text{avg}} = \sum (\text{DBE}_i \times A_i) / \sum A_i$$

$$199 \text{Xc}_{\text{avg}} = \sum (\text{Xc}_i \times A_i) / \sum A_i$$

200 where A_i is the peak abundance for each individual compound i .

201 **3. Results and discussion**

202 **3.1 General characteristics**

203 The main purpose of this study was to tentatively identify and compare the chemical composition
204 of organic compounds in the $\text{PM}_{2.5}$ samples collected in the three Chinese cities: Changchun,
205 Shanghai and Guangzhou during pollution episodes. The number of organic compounds and
206 molecular formulas detected in each city, the peak abundance-weighted average values of
207 molecular mass (MM_{avg}), elemental ratios, DBE, Xc and the isomer number fraction (meaning the
208 percentage of formula numbers that have isomers among all assigned formulas) for each subgroup
209 are listed in Table 1. It should be noted that in this study we focus solely on organic compounds
210 with elevated signal abundances, and thus, presumably rather high concentrations. In contrast to
211 our previous study (Wang et al., 2018), compounds with low concentrations were excluded by
212 increasing the reconstitution volume from 500 μL to 1000 μL , reducing the sample injection volume
213 from 20 μL to 10 μL , and increasing the sample-to-blank ratio from 3 to 10 during data processing.

214 Overall, 416–769 (assigned to 272–415 molecular formulas) and 687–2943 (assigned to 383–679
215 molecular formulas) organic compounds in different samples were determined in ESI⁻ and ESI⁺,
216 respectively. The largest number of organic compounds was observed in Changchun samples in

217 both ESI⁻ and ESI⁺, indicating that OA collected during winter season in Northeast China was
218 more complex compared to urban OA in East and Southeast China. This increased number of
219 compounds can possibly be explained by the large residential coal combustion emissions in winter
220 in North China (Huang et al., 2014; Song et al., 2018; An et al., 2019). In addition, ambient
221 temperatures were lowest during the sampling period in Changchun (i.e., -14 °C to -9 °C, Table
222 S1), which likely led to a decreased boundary layer height and therefore enhanced accumulation of
223 pollutants and enhanced formation of secondary organic aerosol through for example gas-to-
224 particle partitioning.

225 As shown in Table 1, the abundance-weighted average values of MM_{avg} and O/C ratio of the total
226 assigned formulas for Changchun samples detected in negative mode (Changchun⁻) are 169 and
227 0.58, respectively, which are lower than those for Shanghai⁻ ($MM_{avg} = 176$ and $O/C = 0.69$) and
228 for Guangzhou⁻ ($MM_{avg} = 183$ and $O/C = 0.74$). On the contrary, the aromaticity equivalent X_c for
229 organics detected in Changchun⁻, $X_c(\text{Changchun}^-) = 2.13$, is substantially higher than that for
230 Shanghai⁻, $X_c(\text{Shanghai}^-) = 1.92$, and Guangzhou⁻, $X_c(\text{Guangzhou}^-) = 1.65$. These observations
231 indicate that urban OA in Northeast China features a lower degree of oxidation and a higher degree
232 of aromaticity compared to urban OA in East and Southeast China. Furthermore, the relative peak
233 abundance fraction of compounds with $O/C \geq 0.6$, which are considered as highly oxidized
234 compounds (Tu et al., 2016), is 31% in Changchun⁻, and higher in Shanghai⁻ (46%) and
235 Guangzhou⁻ (51%). The different chemical composition of the samples is probably caused by the
236 rather low ambient temperatures and decreased photochemical processing of organic compounds
237 in Northeast China (indicated by the lower solar radiation in Northeast China, see Table S1),
238 slowing down oxidation processes and leading to a larger number of PAHs, which are mainly
239 emitted from coal burning (Huang et al., 2014; Song et al., 2018) or by different
240 biogenic/anthropogenic precursors. In addition, long-range transport of air masses (see the 48 hours
241 back trajectories in Fig. S1) may have a certain effect on the chemical properties of aerosol samples
242 collected in the three cities.

243 Figure 1 shows the reconstructed mass spectra of organic compounds detected in ESI⁻ and ESI⁺.
244 A major fraction organic species detected in ESI⁻ are attributed to CHO⁻ and CHON⁻, accounting
245 for 30–42% and 39–55% in terms of peak abundance, respectively, and comprising 39–45% and
246 23–33% in terms of peak numbers, respectively. This is consistent with previous studies on Chinese
247 urban OA by Wang et al. (2017 and 2018) and Brüggemann et al. (2019). Comparing the organic
248 compounds detected in ESI⁻ for the three cities, 120 formulas were observed in all cities as
249 common formulas (which refer to the compounds detected in all cities with the same molecular

250 formulas and with the same retention times (retention time difference ≤ 0.1 min)) (Fig. 2a),
251 accounting for 29–44% and 57–71% of all assigned formulas in terms of formula numbers and
252 peak abundance, respectively. Despite the above-mentioned differences in chemical composition
253 for OA from Changchun compared to OA from Shanghai and Guangzhou, these results demonstrate
254 that still a large number of common organic compounds exist in Chinese urban OAs collected in
255 different cities, in particular for organics with higher signal abundances. Furthermore, as shown by
256 the pie chart in Fig. 2b, these common formulas are dominated by CHON⁻ and CHO⁻, accounting
257 for 62% and 30% of the total common formulas in terms of peak abundance, respectively.

258 As it is commonly known, ESI exhibits different ionization mechanisms in negative and positive
259 ionization modes. While ESI⁻ is especially sensitive to deprotonatable compounds (e.g., organic
260 acids), ESI⁺ is more sensitive to protonatable compounds (e.g., organic amines) (Ho et al., 2003).
261 Due to the different ionization mechanisms, clear differences were observed in the mass spectra
262 (Fig. 1) and chemical characteristics (Table 1) from ESI⁻ and ESI⁺ measurements. For example,
263 CHO compounds were preferentially detected in ESI⁻, accounting for a relatively large fraction of
264 30–42% of all detected compounds in terms of peak abundance, compared to merely 4–13% for
265 such CHO compounds in ESI⁺. In contrast, CHN compounds were only observed in ESI⁺, yielding
266 a rather large peak abundance fraction of 40–71%. In particular, as can be seen in Fig.1, several
267 peaks of CHN⁺ compounds in Shanghai⁺ and Guangzhou⁺ have much higher abundance compared
268 to other organic species, probably due to their high concentrations and/or high ionization
269 efficiencies in the positive mode. This observation indicates that most CHO compounds with high
270 concentrations are probably organic acids, whereas the majority of CHN compounds likely belong
271 to the group of organic amines, which is in good agreement with previous studies (Lin et al., 2012a;
272 Wang et al., 2017; Wang et al., 2018). Organic compounds in ESI⁺ are dominated by CHN⁺ and
273 CHON⁺ compounds in terms of both peak numbers and peak abundance and these compounds are
274 characterized by rather high H/C ratio and low O/C ratios (Table 1), indicating a low degree of
275 oxidation. The Venn diagram presented for ESI⁺ measurements in Fig. 2a shows that out of a total
276 of 383–679 formulas, 129 formulas were found in samples from all three cities. Such common
277 formulas, thus, account for 19–34% and 30–75% of all assigned formulas in terms of formula
278 numbers and peak abundance, respectively. Among these common formulas, CHN⁺ and CHON⁺
279 exhibit the highest abundance fractions of 72% and 26%, respectively (Fig. 2b).

280 In the following, we will compare and discuss the chemical properties in detail for the three cities,
281 including degrees of oxidation, unsaturation and aromaticity of each organic compound class (i.e.,
282 CHO, CHON, CHN, CHOS and CHONS). It should be noted that the chlorine-containing

283 compounds were not discussed in this study due to the very low MS signal abundance. In addition,
284 since peak abundances for the formula can vary by orders of magnitude, the area of the circles
285 presented in the Figure 3 and Figures 5–7 is proportional to the fourth root of the peak abundance
286 of each formula to reduce the size difference of the circles. For a more detailed comparison, figures
287 with the circle size related to the absolute peak abundances are presented in the SI.

288 3.2 CHO compounds

289 CHO compounds have been widely observed in urban OA, accounting for a substantial fraction
290 (8–67%) of OA (Rincón et al., 2012; Tao et al., 2014; Wang et al., 2017; Wang et al., 2018).
291 Previous studies have shown that a large fraction of CHO compounds in urban OA is composed of
292 organic acids, containing deprotonatable carboxyl functional groups, which are detected
293 preferentially in negative ionization mode when using ESI–MS. As shown in Table 1, a total of
294 346, 164, and 196 CHO– compounds were detected in ESI– in the OA samples collected in
295 Changchun, Shanghai and Guangzhou, accounting for 30%, 40% and 42% of the overall peak
296 abundance in each sample, respectively. Out of all assigned formulas, 47 common CHO– formulas
297 were observed for all cites, accounting for 35–52% and 42–68% of all identified CHO– formulas
298 in terms of formula numbers and peak abundance, respectively.

299 Despite this similarity, OA samples from Changchun– (i.e. in negative ionization mode) exhibit
300 certain differences compared to samples from Shanghai– and Guangzhou–. The average H/C
301 values for CHO– compounds are in a similar range for the three locations (i.e., 0.96–1.10), however,
302 the average O/C values for O/C(Shanghai–) = 0.59 and O/C(Guangzhou–) = 0.65 are rather high
303 compared to the average O/C ratio for Changchun–, O/C(Changchun–) = 0.41. Furthermore, the
304 relative peak abundance fraction of CHO– compounds with O/C ≥ 0.6, which are considered as
305 highly oxidized compounds (Tu et al., 2016), is 14% in Changchun and somewhat higher in
306 Shanghai– (34%) and Guangzhou– (45%). Altogether, these results indicate that CHO– compounds
307 in urban OA from East and Southeast China experienced more intense oxidation and aging
308 processes and/or were affected to a larger degree by biogenic sources.

309 Similarly, as shown in Fig. 3, the abundance-weighted average molecular formulas for CHO–
310 compounds in Changchun–, Shanghai– and Guangzhou– are $C_{8.58}H_{7.86}O_{3.22}$ ($MM_{avg}(\text{Changchun–})$
311 = 162), $C_{8.01}H_{7.27}O_{4.22}$ ($MM_{avg}(\text{Shanghai–})$ = 171) and $C_{7.70}H_{8.04}O_{4.48}$ ($MM_{avg}(\text{Guangzhou–})$ = 172),
312 respectively. Again, these average formulas show that CHO– in Shanghai– and Guangzhou–
313 experienced more intense oxidation processes and/or were affected to a larger degree by biogenic
314 precursors, indicated by the larger abundance-weighted MM_{avg} with a higher degree of oxygenation.

315 In contrast, CHO⁻ compounds from OA samples in Changchun⁻ exhibit a lower abundance-
316 weighted MM_{avg} with a decreased oxygen content.

317 Besides oxygenation, the aromaticity of the detected CHO⁻ compounds exhibits remarkable
318 differences in these three cities. In all cities, the CHO⁻ compounds with high peak abundance were
319 mainly assigned to monoaromatics with $2.5 \leq X_c < 2.7$ (purple circles in Fig. 3) in the region of
320 7–12 carbon atoms per compound and DBE values of 5–7. The relative peak abundance fraction
321 of monoaromatics in total CHO⁻ compounds is 67% in Changchun, which is higher compared to
322 64% in Shanghai and 49% in Guangzhou. In addition, 14% of CHO⁻ compounds in Changchun
323 were identified as polyaromatic compounds with $X_c \geq 2.7$ (red circles in Fig. 3), which is higher
324 than the 8% in Shanghai and 4% in Guangzhou. These observations indicate that CHO⁻ compounds
325 in the three Chinese cities are highly affected by aromatic precursors (e.g., benzene, toluene and
326 naphthalene), in particular for the Changchun aerosol samples.

327 Besides the monoaromatics and polyaromatics, the rest of the detected CHO⁻ compounds were
328 assigned to aliphatic compounds with an X_c lower than 2.5 (grey circles in Fig. 3). Interestingly,
329 these aliphatic compounds account for about 47% of all CHO⁻ compounds for Guangzhou⁻
330 samples in terms of peak abundance, whereas samples from Changchun⁻ and Shanghai⁻ exhibit
331 only rather small fractions of such CHO⁻ compounds, i.e., 19% and 28%, respectively. Such
332 aliphatic compounds are commonly derived from biogenic precursors (Kourtchev et al., 2016) and
333 vehicle emission (Tao et al., 2014; Wang et al., 2017) and/or generated by intense oxidation
334 processes of aromatic precursors, indicating the different biogenic and anthropogenic emission
335 sources and chemical reaction processes for OAs in the three cities.

336 In addition, through the analysis of individual formulas, we find that for the Changchun⁻ samples,
337 formulas of $C_8H_6O_4$, $C_7H_6O_2$, $C_7H_6O_3$, $C_8H_8O_2$, and $C_8H_8O_3$ with DBE values of 6, 5, 5, 5, and 5
338 dominate the assigned CHO formulas with respect to peak abundance. According to previous
339 studies, $C_8H_6O_4$, $C_7H_6O_2$ and $C_7H_6O_3$ are suggested to be phthalic acid, benzoic acid and
340 monohydroxy benzoic acid, respectively, which are derived from naphthalene (Kautzman et al.,
341 2010; Riva et al., 2015; Wang et al., 2017; He et al., 2018; Huang et al., 2019). $C_8H_8O_2$ is likely 4-
342 hydroxy acetophenone, which could be derived from estragole (Pereira et al., 2014), while $C_8H_8O_3$
343 is suggested to be either 4-methoxybenzoic acid generated from estragole (Pereira et al., 2014) or
344 vanillin emitted from biomass burning (Li et al., 2014). For the Shanghai⁻ samples, besides $C_8H_6O_4$,
345 $C_7H_6O_3$ and $C_7H_6O_2$, formulas of $C_6H_8O_7$ and $C_9H_8O_4$ with DBE values of 3 and 6 were observed
346 with high peak abundances. $C_6H_8O_7$ was identified as citric acid in the pollen sample and mountain

347 particle sample in previous studies (Fu et al., 2008; Wang et al., 2009; Jung and Kawamura, 2011)
348 and $C_9H_8O_4$ are probably homophthalic acid derived from e.g. estragole (Pereira et al., 2014). For
349 the Guangzhou- samples, besides the formulas of $C_8H_6O_4$ and $C_6H_8O_7$ discussed above, $C_4H_6O_4$
350 and $C_4H_6O_5$ with low DBE values of two were detected with high abundances and are suggested to
351 be succinic acid and malic acid, respectively (Claeys et al., 2004; Wang et al., 2017).

352 3.3 CHON compounds

353 A large amount of nitrogen-containing organic compounds was detected in these three cities,
354 accounting for 39–55% and 25–47% of total peak abundance detected in ESI- and ESI+,
355 respectively. Out of all assigned formulas, 45 common CHON- and 62 common CHON+ formulas
356 were observed in all cities, accounting for 65–82% and 25–44% of all CHON compounds detected
357 in ESI- and ESI+ in terms of peak abundance, respectively. It indicates that a large amount of
358 CHON compounds in all three Chinese cities show similar properties of chemical composition.

359 The CHON compounds were further classified into different subgroups according to their O/N
360 ratios (Fig. 4 for CHON- and Fig. S3 for CHON+) or according to the number of nitrogen atoms
361 in their molecular formulas (see Fig. S4 for CHON- and S5 for CHON+). As shown in Fig. 4, the
362 majority (84–96% in terms of peak abundance) of CHON- compounds exhibited O/N ratios ≥ 3 ,
363 allowing the assignment of one nitro ($-NO_2$) or nitrooxy ($-ONO_2$) group for these formulas, which
364 are preferentially ionized in ESI- mode (Lin et al., 2012b; Wang et al., 2017; Song et al., 2018;
365 Wang et al., 2018). CHON- formulas with O/N ratios ≥ 4 suggest the presence of further
366 oxygenated functional groups, such as a hydroxyl group ($-OH$) or a carbonyl group ($C=O$). In
367 terms of peak abundance, 59% of CHON- compounds observed in Guangzhou- exhibited formulas
368 with O/N ratios ≥ 4 , which is higher than 51% in Changchun- and 45% in Shanghai-, indicating
369 that CHON- compounds in Southeast China show a higher degree of oxidation compared to those
370 in Northeast and East China. Not surprisingly, CHON+ compounds generally exhibit lower O/N
371 ratios (Fig. S3), as they probably contain reduced nitrogen functional group (e.g., amines) which
372 are preferably detected in ESI+. As shown in Fig. S3, CHON+ compounds with O/N ratio of 1 are
373 dominant in Changchun+, whereas CHON+ compounds in Shanghai+ and Guangzhou+ show a
374 broader range of O/N ratios from 1 to 3. Moreover, the average O/C ratios (0.27–0.45) in Shanghai+
375 and Guangzhou+ (Table 1) are much greater than that (0.19) in Changchun+. Consistent with the
376 observations for CHO compounds, these results indicate again that CHON+ compounds in the OA
377 of East and Southeast China experienced more intensive photooxidation and/or were affected to a
378 larger degree by biogenic precursors.

379 Figure 5 shows the DBE versus C number of CHON⁻ compounds for the three cities. The majority
380 of CHON⁻ compounds lie in the region of 5–15 C atoms and 3–10 DBEs. 67% of CHON⁻
381 compounds in terms of peak abundance were assigned to mono or polyaromatics in Shanghai⁻,
382 which is higher than 52% in Guangzhou⁻ and 55% in Changchun⁻. It indicates that CHON⁻
383 compounds are dominated with aromatic compounds in all cities, while relatively higher peak
384 abundance weighted fraction of aromatic CHON⁻ compounds were observed in Shanghai. The
385 peak abundance-weighted average molecular formulas for CHON⁻ compounds in Changchun⁻,
386 Shanghai⁻ and Guangzhou⁻ are C_{7.10}H_{6.76}O_{3.56}N_{1.03}, C_{7.07}H_{6.03}O_{3.80}N_{1.24} and C_{7.12}H_{6.36}O_{3.99}N_{1.24},
387 respectively, showing that CHON⁻ formulas in Shanghai⁻ and Guangzhou⁻ contain more O and
388 N atoms on average than those for Changchun⁻. Formulas of C₆H₅O₃N₁, C₆H₅O₄N₁, C₇H₇O₃N₁,
389 C₇H₇O₄N₁, C₈H₉O₃N₁, and C₈H₉O₄N₁ were detected with the highest abundance in all cities. These
390 molecular formulas are in line with nitrophenol or nitrocatechol analogs, which have been identified
391 in a previous urban OA study (Wang et al., 2017). Furthermore, these nitrooxy-aromatic
392 compounds were shown to enhance light absorbing properties of OA (Laskin et al., 2015; Lin et al.,
393 2015). In addition, it should be noted that the X_c values for C₆H₅O₄N₁, C₇H₇O₄N₁ and C₈H₉O₄N₁
394 were calculated to be lower than 2.5, suggesting that the fraction of aromatics in CHON⁻
395 compounds was underestimated. This is because that for nitrocatechol analogs with formulas of
396 C₆H₅O₄N₁, C₇H₇O₄N₁ and C₈H₉O₄N₁, only one oxygen atom is involved in the π-bond structure
397 corresponding to the p value of 0.25 in the X_c calculation equation, which is lower than the p value
398 of 0.5 applied for the X_c calculation in this study. The diagram of DBE versus C number for
399 CHON⁺ compounds observed in the three locations (presented in Fig. S7 in SI) shows that more
400 aromatic CHON⁺ compounds with relatively lower degree of oxidation were assigned in
401 Changchun⁺ samples compared to Shanghai⁺ and Guangzhou⁺ samples.

402 **3.4 CHN⁺ compounds**

403 696 CHN⁺ compounds were detected in Changchun⁺ samples in ESI⁺, which is higher than in
404 Shanghai⁺ (253) and Guangzhou (205). These CHN⁺ compounds are likely assignable to amines
405 according to previous studies (Rincón et al., 2012; Wang et al., 2017; Wang et al., 2018). The
406 number of CHN⁺ compounds accounts for 24%, 36% and 30% of the total organic compounds in
407 Changchun⁺, Shanghai⁺ and Guangzhou⁺, respectively, whereas the peak abundance of these
408 compounds accounts for 40%, 71% and 62%, respectively. The majority (> 97% in terms of peak
409 abundance) of CHN⁺ compounds have one or two nitrogen atoms in their molecular formulas (see
410 Fig. S9). Comparing the CHN⁺ compounds for the three cities, 51 common CHN⁺ formulas were
411 observed in all cities, which contribute to as much as 43–89% of the total abundance of CHN⁺

412 formulas. This large percentage indicates that CHN⁺ compounds with presumably high
413 concentrations in Changchun⁺, Shanghai⁺ and Guangzhou⁺ exhibit similar chemical composition.
414 However, again OA samples from Changchun show some distinct differences to samples from
415 Guangzhou and Shanghai.

416 A van Krevelen diagram of CHN⁺ compounds detected in the three samples is shown in Fig. 6,
417 illustrating H/C ratios as a function of N/C ratio. In this plot, major parts of the CHN⁺ compounds
418 are found in a region, which is constraint by H/C ratios between 0.5 and 2 and N/C ratios lower
419 than 0.5. Moreover, the pie charts show that the majority (83–87% in terms of peak abundance and
420 72–90% in terms of peak numbers) of these CHN⁺ compounds can be assigned to mono- and
421 polyaromatics with $X_c \geq 2.5$. In addition, as shown in Table 1, the average DBE and X_c values of
422 CHN⁺ compounds are the highest among all organic species. These observations imply that CHN⁺
423 compounds exhibit the highest degree of aromaticity of all organics in the Chinese urban OA
424 samples, which is consistent with previous studies (Lin et al., 2012b; Rincón et al., 2012; Wang et
425 al., 2018). Polyaromatic compounds with $X_c \geq 2.7$ are displayed in the lower left corner of the
426 van Krevelen diagram, accounting for 41% in terms of peak abundance (48% in terms of peak
427 numbers) of CHN⁺ compounds detected in Changchun⁺, but merely for 9–10% in terms of peak
428 abundance (27–31% in terms of peak numbers) in Shanghai⁺ and Guangzhou⁺. For example,
429 formulas of C₁₁H₁₁N₁ ($X_c = 2.7$), C₁₀H₉N₁ ($X_c = 2.7$), and C₁₂H₁₃N₁ ($X_c = 2.7$), which are assigned
430 to be naphthalene core structure-containing compounds, have relatively higher abundance in
431 Changchun⁺ than in Shanghai⁺ and Guangzhou⁺. Moreover, the average DBE and X_c values of
432 CHN⁺ compounds (see Table 1) in Changchun⁺ are substantially higher than those in Shanghai⁺
433 and Guangzhou⁺, further indicating that CHN⁺ compounds in Changchun⁺ show a higher degree
434 of aromaticity, which can be caused by large coal combustion emissions in the winter in Changchun.
435 Remarkably, as can be seen in Fig. 6, the abundance of CHN⁺ compounds in Changchun⁺
436 distributes evenly among different individual CHN⁺ compounds, while in Shanghai⁺ and
437 Guangzhou⁺ they are dominated by the formula of C₁₀H₁₄N₂ (the biggest purple circle in Fig. 6)
438 with DBE value of 5, which probably has high concentration and/or high ionization efficiency in
439 the positive ESI mode. According to a previous smog chamber study (Laskin et al., 2010), most
440 CHN⁺ aromatics are probably generated from biomass burning through the addition of reduced
441 nitrogen (e.g., NH₃) to the organic molecules via imine formation reaction, indicating that biomass
442 burning probably made a certain contribution to the formation of CHN⁺ compounds observed in
443 the three urban OA samples in our study.

444 3.5 CHOS⁻ compounds

445 In this study, 75–155 CHOS⁻ compounds were observed, accounting for 10%, 12% and 14% of
446 the total peak abundance of all organics in Changchun⁻, Shanghai⁻ and Guangzhou⁻, respectively.
447 Around 89–96% of these CHOS⁻ compounds were found to fulfill the O/S \geq 4 criterion allowing
448 the assignment of at least one –OSO₃H functional group, and thus, a tentative classification to
449 organosulfates (OSs) (Lin et al., 2012a; Lin et al., 2012b; Tao et al., 2014; Wang et al., 2016; Wang
450 et al., 2017; Wang et al., 2018; Wang et al., 2019a). OSs were shown to affect the surface activity
451 and hygroscopic properties of the aerosol particles, leading to potential impacts on climate (Hansen
452 et al., 2015; Wang et al., 2019a). Out of all formulas, 23 common CHOS⁻ formulas were detected
453 for the three sample locations, accounting for 28%, 58% and 52% of the CHOS⁻ peak abundance
454 in Changchun⁻, Shanghai⁻ and Guangzhou⁻, respectively. However, 40 common CHOS⁻
455 formulas were found between Shanghai⁻ and Guangzhou⁻, accounting for 60–65% and 78–81%
456 in terms of the CHOS⁻ formula numbers and peak abundance, respectively. This indicates that the
457 chemical composition of the major CHOS⁻ compounds of Shanghai⁻ and Guangzhou⁻ are quite
458 similar, while they show substantial chemical differences for samples from Changchun⁻.

459 Figure 7 shows the DBEs as a function of carbon number for all CHOS⁻ compounds detected for
460 the three cities. The CHOS⁻ compounds exhibit a DBE range from 0 to 10 and carbon number
461 range of 2–15. However, the majority of CHOS⁻ compounds with elevated peak abundances
462 concentrate in a region with rather low DBE values of 0–5. The average H/C ratios of CHOS⁻
463 compounds are in the range of 1.56–1.85, and thus, higher than for any other compound class,
464 whereas the average DBE values of 1.71–2.55 are the lowest among all classes. This indicates that
465 CHOS⁻ compounds in the OA from the three Chinese cities are characterized by a low degree of
466 unsaturation. Moreover, the pie charts in Fig. 7 show that aliphatic compounds with X_c \leq 2.5 are
467 dominant in CHOS⁻ compounds with a fraction of 96–99% in terms of peak abundance, which is
468 substantially higher than that (13–48%) for CHO, CHON and CHN species. Aliphatic CHOS⁻
469 compounds with C \leq 10 can be formed from biogenic and/or anthropogenic precursors (Hansen
470 et al., 2014; Glasius et al., 2018; Wang et al., 2019a), such as C₂H₄O₆S₁ (derived from glyoxal)
471 (Lim et al., 2010; McNeill et al., 2012), C₃H₆O₆S₁ (derived from isoprene) (Surratt et al., 2007) and
472 C₈H₁₆O₄S₁ (derived from α -pinene). However, more CHOS⁻ compounds with C > 10 and with
473 DBEs lower than 1 are observed in Changchun⁻, such as C₁₄H₂₈O₅S₁, C₁₃H₂₆O₅S₁, C₁₂H₂₄O₅S₁,
474 C₁₁H₂₂O₅S₁ and C₁₁H₂₀O₆S₁. These high-carbon-number-containing CHOS⁻ compounds are likely
475 formed from long-alkyl-chain compounds with less oxygenated functional groups, which were
476 previously suggested to be emitted from traffic (Tao et al., 2014) or derived from sesquiterpene
477 emissions (Brüggemann et al., 2019). However, as sesquiterpene emissions can be expected to be

478 very low in wintertime at Changchun, the presence of these compounds further underlines the
479 strong impact of anthropogenic emissions on CHOS⁻ formation in Changchun⁻. In this study,
480 (O-3S)/C ratio was used instead of traditional O/C ratio to present the oxidation state of CHOS⁻
481 compounds, since the sulfate functional group contains three more oxygen atoms than common
482 oxygen-containing groups (e.g., hydroxyl and carbonyl), which makes no contribution to the
483 oxidation state of the carbon backbone of the CHOS⁻ compounds. Comparing average values for
484 H/C, (O-3S)/C and DBEs of CHOS⁻ for the three sample locations (see Table 1), we find that the
485 H/C ratios (1.85) and (O-3S)/C ratios (0.61-0.71) for Shanghai⁻ and Guangzhou⁻ samples are
486 larger than those for Changchun⁻ samples (H/C = 1.56 and (O-3S)/C = 0.52), whereas the DBE
487 values (1.71-1.79) in Shanghai⁻ and Guangzhou⁻ are lower than those for Changchun⁻ (2.55).
488 These observations indicate that CHOS⁻ compounds in urban OA from Northeast China are less
489 oxidized but more unsaturated compared to those in East and Southeast China, likely due to
490 enhanced emissions from residential heating during winter in North China.

491 **3.6 CHONS compounds**

492 4-5% of the total organics detected in ESI⁻ were identified as CHONS⁻ compounds in terms of
493 peak abundance. In contrast, CHONS⁺ compounds account merely for 0.3-1% of all organics
494 detected in ESI⁺. The average MM_{avg} of the CHONS⁻ compounds for the three sample locations
495 ranges from 214 to 293 Da, generally showing larger molecular masses than compounds of any
496 other class because of the likely presence of both nitrate and sulfate functional groups. In total, only
497 5 common CHONS⁻ formulas were detected for all three sample locations, accounting for 4%, 21%
498 and 20% of the CHONS⁻ peak abundance in Changchun⁻, Shanghai⁻ and Guangzhou⁻,
499 respectively. As already observed for other compound classes, these percentages imply that the
500 CHONS⁻ compounds in urban OA of Shanghai⁻ and Guangzhou⁻ exhibit a rather similar chemical
501 composition, whereas such compounds are different for Changchun⁻.

502 In the OA samples of Shanghai⁻ and Guangzhou⁻, 78-87% of CHONS⁻ compounds in terms of
503 peak abundance have 7 or more O atoms in their formulas, allowing the assignment of one -OSO₃H
504 and one -NO₃ functional groups in the molecular structures, thus, classifying them as potential
505 nitrooxy-organosulfates. In contrast to Shanghai⁻ and Guangzhou⁻, only 26% of CHONS⁻
506 compounds were assigned to such nitrooxy-organosulfates for Changchun⁻, indicating that most
507 of the N atoms in the CHONS⁻ compounds are present in a reduced oxidation state, e.g., in the
508 form of amines. The average DBE and X_c values of CHONS⁻ compounds in Shanghai⁻ and
509 Guangzhou⁻ are 3.3-3.45 and 0.43-0.44, respectively. Again these values differ for the

510 Changchun– samples with an increased average DBE of 3.75 and an average Xc of 1.06, indicating
511 that CHONS- compounds in Changchun– possess on average a higher degree of unsaturation and
512 aromaticity compared to such compounds in Shanghai– and Guangzhou– samples. Interestingly,
513 the compound with formula $C_{10}H_{17}O_7NS$ has the highest relative peak abundance (32%) in
514 Shanghai– and Guangzhou–, whereas in Changchun– the compound with formula $C_2H_3O_4NS$ is
515 dominant. $C_{10}H_{17}O_7NS$ has previously been identified as mononitrate organosulfate generated from
516 α/β -pinene (Inuma et al., 2007; Surratt et al., 2008; Lin et al., 2012b; Wang et al., 2017), while
517 $C_2H_3O_4NS$ may be assigned as a cyanogroup-containing sulfate. This observation is comparable to
518 our previous study (Wang et al., 2019a), which found that $C_{10}H_{17}O_7NS$ was dominant for CHONS–
519 compounds in low-concentration aerosol samples collected in Beijing (China) and Mainz
520 (Germany). Consistently, a $C_2H_3O_4NS$ compound had the highest abundance among CHONS–
521 compounds in polluted Beijing aerosol samples. This agreement can be explained by the adjacent
522 locations of Beijing (39.99° N, 116.39° E) and Changchun (43.54° N, 125.13° E) and similar
523 residential heating patterns by coal combustion during wintertime. In conclusion, these results
524 further demonstrate that the precursors for CHONS– compounds in Shanghai– and Guangzhou–
525 are different from those in Changchun–, which is probably due to differences in anthropogenic
526 emissions.

527 **4 Conclusion**

528 The molecular composition of the organic fraction of $PM_{2.5}$ samples collected in three Chinese
529 megacities (Changchun, Shanghai and Guangzhou) was investigated using a UHPLC-Orbitrap
530 mass spectrometer. In total, 416–769 (ESI–) and 687–2943 (ESI+) organic compounds were
531 observed and separated into five subgroups: CHO, CHN, CHON, CHOS and CHONS. Specifically,
532 120 common formulas were detected in ESI– and 129 common formulas in ESI+ for all sample
533 locations, accounting for 57–71% and 30–75% in terms of peak abundance, respectively. Overall,
534 we found that urban OA in Changchun, Shanghai and Guangzhou shows a quite similar chemical
535 composition for organic compounds of high concentrations. The majority of these organic species
536 was assigned to mono-aromatic or poly-aromatic compounds, indicating that anthropogenic
537 emissions are the major source for urban OA in all three cities.

538 Despite the chemical similarity of the three sample locations for organic compounds in urban OA,
539 remarkable differences were found in chemical composition of the remaining particle constituents,
540 in particular for OA samples from Changchun. In general, a larger amount of polyaromatics was
541 observed for Changchun samples, most likely due to emissions from coal combustion during

542 wintertime residential heating period. Moreover, the peak abundance-weighted average DBE and
543 average Xc values of the total organic compounds in Changchun were found to be larger than those
544 for Shanghai and Guangzhou, showing that organic compounds in Changchun possess a higher
545 degree of unsaturation and aromaticity. For average H/C and O/C ratios a similar trend was
546 observed. While average H/C and O/C ratios detected in ESI⁻ were found to be highest for
547 Guangzhou samples, relatively lower values were observed for Shanghai and Changchun samples,
548 indicating that OA collected in lower latitude regions of China experiences more intense
549 photochemical oxidation processes and/or are affected to a larger degree by biogenic sources.

550 **5 Limitations**

551 In this study, we used the peak abundance-weighted method to illustrate the difference in chemical
552 formulas assigned by Orbitrap mass spectrometry. This comparison was made based on the
553 assumption that the measured organic compounds have same peak abundance response in the mass
554 spectrometer. However, this assumption can bring some uncertainties because the ionization
555 efficiencies vary between different compounds (Schmidt et al., 2006; Leito et al., 2008; Perry et al.,
556 2008; Krueve et al., 2014). For example, the ionization efficiencies of nitrophenol species detected
557 in negative ESI mode can vary by a large degree depending on the position of the substituents at
558 the nitrobenzene ring (Schmidt et al., 2006; Krueve et al., 2014) and the ionization efficiencies of
559 carboxylic acids can also vary by several orders of magnitude depending on the structures (Krueve
560 et al., 2014). Nonetheless, it is a challenging analytical task to identify and quantify all compounds
561 in ambient OA due to the high chemical complexity of OA and the limits in authentic standards of
562 OA. Despite the inherent uncertainties, the peak abundance-weighted comparison of molecular
563 formulas provides an overview of the difference in chemical composition of OA in these three
564 representative Chinese cities. In particular, the chemical formulas assigned in this study can be
565 validated in future studies by authentic standards and the difference in ionization efficiencies can
566 be further evaluated.

567

568 **Author contributions.** RJH, TH and KW conducted the study design. LY, HN, JG and MW
569 collected the PM_{2.5} filter samples. KW and YZ carried out the experimental work and data analysis.
570 KW wrote the manuscript. KW, TH, RJH, M. Brüggemann, YZ, JH, M. Bilde and MG interpreted
571 data and edited the manuscript. All authors commented on and discussed the manuscript.

572 **Competing interests.** The authors declare that they have no conflict of interest.

573 **Acknowledgements.** This study was supported by the National Natural Science Foundation of
574 China (NSFC, Grant No. 41925015, No. 91644219 and No. 41877408), the Chinese Academy of
575 Sciences (No. ZDBS-LY-DQC001), the National Key Research and Development Program of
576 China (No. 2017YFC0212701), and the German Research Foundation (Deutsche
577 Forschungsgemeinschaft, DFG) under Grant No. INST 247/664-1 FUGG. K. Wang and Y. Zhang
578 acknowledge the scholarship from Chinese Scholarship Council (CSC) and Max Plank Graduate
579 Center with Johannes Gutenberg University of Mainz (MPGC) and thanks Prof. Ulrich Pöschl, Dr.
580 Christopher J. Kampf and Dr. Yafang Cheng for their helpful suggestion on this study. K. Wang
581 also thanks Dr. Huanfeng Dong from Zhejiang University for the great support on the programming
582 of data process.

583
584
585
586
587
588
589
590
591
592
593
594
595
596
597
598
599
600
601
602
603
604
605
606
607
608
609
610
611
612
613
614
615
616
617
618
619
620

621 **References**

- 622
- 623 An, Z., Huang, R. J., Zhang, R., Tie, X., Li, G., Cao, J., Zhou, W., Shi, Z., Han, Y., Gu, Z., and Ji, Y.: Severe
624 haze in northern China: A synergy of anthropogenic emissions and atmospheric processes, *Proc Natl Acad*
625 *Sci U S A*, 116, 8657-8666, 10.1073/pnas.1900125116, 2019.
- 626 Brüggemann, M., Poulain, L., Held, A., Stelzer, T., Zuth, C., Richters, S., Mutzel, A., van Pinxteren, D.,
627 Inuma, Y., Katkevica, S., Rabe, R., Herrmann, H., and Hoffmann, T.: Real-time detection of highly
628 oxidized organosulfates and BSOA marker compounds during the F-BEACH 2014 field study, *Atmos.*
629 *Chem. Phys.*, 17, 1453-1469, 10.5194/acp-17-1453-2017, 2017.
- 630 Brüggemann, M., van Pinxteren, D., Wang, Y., Yu, J. Z., and Herrmann, H.: Quantification of known and
631 unknown terpenoid organosulfates in PM10 using untargeted LC-HRMS/MS: contrasting summertime
632 rural Germany and the North China Plain, *Environmental Chemistry*, -, <https://doi.org/10.1071/EN19089>,
633 2019.
- 634 Claeys, M., Graham, B., Vas, G., Wang, W., Vermeylen, R., Pashynska, V., Cafmeyer, J., Guyon, P., Andre,
635 M., Artaxo, P., and Maenhaut, W.: Formation of secondary organic aerosol through photooxidation of
636 isoprene, *Science*, 303, 1173-1175, 10.1126/science.1092805, 2004.
- 637 Daellenbach, K. R., Kourtchev, I., Vogel, A. L., Bruns, E. A., Jiang, J., Petäjä, T., Jaffrezo, J.-L., Aksoyoglu,
638 S., Kalberer, M., Baltensperger, U., El Haddad, I., and Prévôt, A. S. H.: Impact of anthropogenic and
639 biogenic sources on the seasonal variation in the molecular composition of urban organic aerosols: a field
640 and laboratory study using ultra-high-resolution mass spectrometry, *Atmospheric Chemistry and Physics*,
641 19, 5973-5991, 10.5194/acp-19-5973-2019, 2019.
- 642 Ding, X., Zhang, Y.-Q., He, Q.-F., Yu, Q.-Q., Shen, R.-Q., Zhang, Y., Zhang, Z., Lyu, S.-J., Hu, Q.-H., Wang,
643 Y.-S., Li, L.-F., Song, W., and Wang, X.-M.: Spatial and seasonal variations of secondary organic aerosol
644 from terpenoids over China, *J. geophys. Res.-Atoms.*, 121, 14661-14678, doi:10.1002/2016JD025467,
645 2016.
- 646 Elzein, A., Dunmore, R. E., Ward, M. W., Hamilton, J. F., and Lewis, A. C.: Variability of polycyclic
647 aromatic hydrocarbons and their oxidative derivatives in wintertime Beijing, China, *Atmospheric*
648 *Chemistry and Physics*, 19, 8741-8758, 10.5194/acp-19-8741-2019, 2019.
- 649 Fleming, L. T., Lin, P., Laskin, A., Laskin, J., Weltman, R., Edwards, R. D., Arora, N. K., Yadav, A.,
650 Meinardi, S., Blake, D. R., Pillarisetti, A., Smith, K. R., and Nizkorodov, S. A.: Molecular composition
651 of particulate matter emissions from dung and brushwood burning household cookstoves in Haryana,
652 India, *Atmos. Chem. Phys.*, 18, 2461-2480, 10.5194/acp-18-2461-2018, 2018.
- 653 Fu, P., Kawamura, K., Okuzawa, K., Aggarwal, S. G., Wang, G., Kanaya, Y., and Wang, Z.: Organic
654 molecular compositions and temporal variations of summertime mountain aerosols over Mt. Tai, North
655 China Plain, *J. Geophys. Res.*, 113, 10.1029/2008jd009900, 2008.
- 656 Glasius, M., Hansen, A. M. K., Claeys, M., Henzing, J. S., Jedynska, A. D., Kasper-Giebl, A., Kistler, M.,
657 Kristensen, K., Martinsson, J., Maenhaut, W., Nøjgaard, J. K., Spindler, G., Stenström, K. E., Swietlicki,
658 E., Szidat, S., Simpson, D., and Yttri, K. E.: Composition and sources of carbonaceous aerosols in
659 Northern Europe during winter, *Atmos. Environ.*, 173, 127-141, 10.1016/j.atmosenv.2017.11.005, 2018.
- 660 Hansen, A. M. K., Kristensen, K., Nguyen, Q. T., Zare, A., Cozzi, F., Noejgaard, J. K., Skov, H., Brandt, J.,
661 Christensen, J. H., Strom, J., Tunved, P., Krejci, R., and Glasius, M.: Organosulfates and organic acids in
662 Arctic aerosols: speciation, annual variation and concentration levels, *Atmos. Chem. Phys.*, 14, 7807-
663 7823, <https://doi.org/10.5194/acp-14-7807-2014>, 2014.
- 664 Hansen, A. M. K., Hong, J., Raatikainen, T., Kristensen, K., Ylisirniö, A., Virtanen, A., Petäjä, T., Glasius,
665 M., and Prisle, N. L.: Hygroscopic properties and cloud condensation nuclei activation of limonene-
666 derived organosulfates and their mixtures with ammonium sulfate, *Atmos. Chem. Phys.*, 15, 14071-14089,
667 <https://doi.org/10.5194/acp-15-14071-2015>, 2015.
- 668 He, X., Huang, X. H. H., Chow, K. S., Wang, Q., Zhang, T., Wu, D., and Yu, J. Z.: Abundance and Sources
669 of Phthalic Acids, Benzene-Tricarboxylic Acids, and Phenolic Acids in PM2.5 at Urban and Suburban
670 Sites in Southern China, *ACS Earth and Space Chemistry*, 2, 147-158,
671 10.1021/acsearthspacechem.7b00131, 2018.
- 672 Ho, C. S., Lam, C. W. K., Chan, M. H. M., Cheung, R. C. K., Law, L. K., Suen, M. W. M., and Tai, H. L.:
673 Electrospray ionisation mass spectrometry: principles and clinical application, *Clin. Biochem. Rev.*, 24,
674 10, 2003.
- 675 Hoffmann, T., Huang, R. J., and Kalberer, M.: Atmospheric analytical chemistry, *Anal. Chem.*, 83, 4649-

676 4664, 10.1021/ac2010718, 2011.

677 Huang, G., Liu, Y., Shao, M., Li, Y., Chen, Q., Zheng, Y., Wu, Z., Liu, Y., Wu, Y., Hu, M., Li, X., Lu, S.,

678 Wang, C., Liu, J., Zheng, M., and Zhu, T.: Potentially Important Contribution of Gas-Phase Oxidation of

679 Naphthalene and Methylanthalene to Secondary Organic Aerosol during Haze Events in Beijing,

680 *Environ Sci Technol*, 53, 1235-1244, 10.1021/acs.est.8b04523, 2019.

681 Huang, R. J., Zhang, Y., Bozzetti, C., Ho, K. F., Cao, J. J., Han, Y., Daellenbach, K. R., Slowik, J. G., Platt,

682 S. M., Canonaco, F., Zotter, P., Wolf, R., Pieber, S. M., Bruns, E. A., Crippa, M., Ciarelli, G., Piazzalunga,

683 A., Schwikowski, M., Abbaszade, G., Schnelle-Kreis, J., Zimmermann, R., An, Z., Szidat, S.,

684 Baltensperger, U., El Haddad, I., and Prevot, A. S.: High secondary aerosol contribution to particulate

685 pollution during haze events in China, *Nature*, 514, 218-222, 10.1038/nature13774, 2014.

686 Huang, R. J., Cao, J. J., and Worsnop, D.: Sources and Chemical Composition of Particulate Matter During

687 Haze Pollution Events in China, in: *Air pollution in Eastern Asia: an integrated perspective*, edited by

688 Bouarar, I., Wang, X. M., and Brasseur, G. P., Springer, Cham, Switzerland, 49-68, 2017.

689 Iinuma, Y., Müller, C., Berndt, T., Böge, O., Claeys, M., and Herrmann, H.: Evidence for the existence of

690 organosulfates from β -pinene ozonolysis in ambient secondary organic aerosol, *Environ. Sci. Technol.*,

691 41, 6678-6683, 10.1021/es070938t, 2007.

692 Jung, J., and Kawamura, K.: Enhanced concentrations of citric acid in spring aerosols collected at the Gosan

693 background site in East Asia, *Atmos. Environ.*, 45, 5266-5272, 10.1016/j.atmosenv.2011.06.065, 2011.

694 Kautzman, K. E., Surratt, J. D., Chan, M. N., Chan, A. W., Hersey, S. P., Chhabra, P. S., Dalleska, N. F.,

695 Wennberg, P. O., Flagan, R. C., and Seinfeld, J. H.: Chemical composition of gas- and aerosol-phase

696 products from photooxidation of naphthalene, *J. Phys. Chem. A*, 114, 913-934, 10.1021/jp908530s, 2010.

697 Kind, T., and Fiehn, O.: Seven Golden Rules for heuristic filtering of molecular formulas obtained by

698 accurate mass spectrometry, *BMC Bioinformatics*, 8, 10.1186/1471-2105-8-105, 2007.

699 Kourtchev, I., O'Connor, I. P., Giorio, C., Fuller, S. J., Kristensen, K., Maenhaut, W., Wenger, J. C., Sodeau,

700 J. R., Glasius, M., and Kalberer, M.: Effects of anthropogenic emissions on the molecular composition of

701 urban organic aerosols: An ultrahigh resolution mass spectrometry study, *Atmo. Environ.*, 89, 525-532,

702 10.1016/j.atmosenv.2014.02.051, 2014.

703 Kourtchev, I., Godoi, R. H. M., Connors, S., Levine, J. G., Archibald, A. T., Godoi, A. F. L., Paralovo, S. L.,

704 Barbosa, C. G. G., Souza, R. A. F., Manzi, A. O., Seco, R., Sjostedt, S., Park, J.-H., Guenther, A., Kim,

705 S., Smith, J., Martin, S. T., and Kalberer, M.: Molecular composition of organic aerosols in central

706 Amazonia: an ultra-high-resolution mass spectrometry study, *Atmos. Chem. Phys.*, 16, 11899-11913,

707 <https://doi.org/10.5194/acp-16-11899-2016>, 2016.

708 Kruve, A., Kaupmees, K., Liigand, J., and Leito, I.: Negative electrospray ionization via deprotonation:

709 predicting the ionization efficiency, *Anal Chem*, 86, 4822-4830, 10.1021/ac404066v, 2014.

710 Laskin, A., Laskin, J., and Nizkorodov, S. A.: Chemistry of atmospheric brown carbon, *Chem. Rev.*, 115,

711 4335-4382, 10.1021/cr5006167, 2015.

712 Laskin, J., Laskin, A., Roach, P. J., Slysz, G. W., Anderson, G. A., Nizkorodov, S. A., Bones, D. L., and

713 Nguyen, L. Q.: High-Resolution Desorption Electrospray Ionization Mass Spectrometry for Chemical

714 Characterization of Organic Aerosols, *Anal. Chem.*, 82, 2048-2058, 10.1021/ac902801f, 2010.

715 Laskin, J., Laskin, A., and Nizkorodov, S. A.: Mass Spectrometry Analysis in Atmospheric Chemistry, *Anal.*

716 *Chem.*, 90, 166-189, 10.1021/acs.analchem.7b04249, 2018.

717 Lee, A., Goldstein, A. H., Kroll, J. H., Ng, N. L., Varutbangkul, V., Flagan, R. C., and Seinfeld, J. H.: Gas-

718 phase products and secondary aerosol yields from the photooxidation of 16 different terpenes, *J. Geophys.*

719 *Res.*, 111, 10.1029/2006jd007050, 2006.

720 Leito, I., Herodes, K., Huopolainen, M., Virro, K., Kunnapas, A., Kruve, A., and Tanner, R.: Towards the

721 electrospray ionization mass spectrometry ionization efficiency scale of organic compounds, *Rapid*

722 *Commun Mass Spectrom*, 22, 379-384, 10.1002/rcm.3371, 2008.

723 Li, Y. J., Huang, D. D., Cheung, H. Y., Lee, A. K. Y., and Chan, C. K.: Aqueous-phase photochemical

724 oxidation and direct photolysis of vanillin – a model compound of methoxy phenols from biomass burning,

725 *Atmospheric Chemistry and Physics*, 14, 2871-2885, 10.5194/acp-14-2871-2014, 2014.

726 Lim, Y. B., Tan, Y., Perri, M. J., Seitzinger, S. P., and Turpin, B. J.: Aqueous chemistry and its role in

727 secondary organic aerosol (SOA) formation, *Atmos. Chem. Phys.*, 10, 10521-10539, 10.5194/acp-10-

728 10521-2010, 2010.

729 Lin, P., Rincon, A. G., Kalberer, M., and Yu, J. Z.: Elemental composition of HULIS in the Pearl River Delta

730 Region, China: results inferred from positive and negative electrospray high resolution mass

731 spectrometric data, *Environ. Sci. Technol.*, 46, 7454-7462, 10.1021/es300285d, 2012a.

732 Lin, P., Yu, J. Z., Engling, G., and Kalberer, M.: Organosulfates in humic-like substance fraction isolated

733 from aerosols at seven locations in East Asia: a study by ultra-high-resolution mass spectrometry, *Environ.*

734 *Sci. Technol.*, 46, 13118-13127, 10.1021/es303570v, 2012b.

735 Lin, P., Laskin, J., Nizkorodov, S. A., and Laskin, A.: Revealing Brown Carbon Chromophores Produced in

736 Reactions of Methylglyoxal with Ammonium Sulfate, *Environ. Sci. Technol.*, 49, 14257-14266,

737 10.1021/acs.est.5b03608, 2015.

738 McNeill, V. F., Woo, J. L., Kim, D. D., Schwier, A. N., Wannell, N. J., Sumner, A. J., and Barakat, J. M.:

739 Aqueous-phase secondary organic aerosol and organosulfate formation in atmospheric aerosols: a

740 modeling study, *Environ Sci Technol*, 46, 8075-8081, 10.1021/es3002986, 2012.

741 Ning, C., Gao, Y., Zhang, H., Yu, H., Wang, L., Geng, N., Cao, R., and Chen, J.: Molecular characterization

742 of dissolved organic matters in winter atmospheric fine particulate matters (PM_{2.5}) from a coastal city of

743 northeast China, *Sci Total Environ*, 689, 312-321, 10.1016/j.scitotenv.2019.06.418, 2019.

744 Nizkorodov, S. A., Laskin, J., and Laskin, A.: Molecular chemistry of organic aerosols through the

745 application of high resolution mass spectrometry, *Phys. Chem. Chem. Phys.*, 13, 3612-3629,

746 10.1039/c0cp02032j, 2011.

747 Noziere, B., Kalberer, M., Claeys, M., Allan, J., D'Anna, B., Decesari, S., Finessi, E., Glasius, M., Grgic, I.,

748 Hamilton, J. F., Hoffmann, T., Iinuma, Y., Jaoui, M., Kahnt, A., Kampf, C. J., Kourtchev, I., Maenhaut,

749 W., Marsden, N., Saarikoski, S., Schnelle-Kreis, J., Surratt, J. D., Szidat, S., Szmigielski, R., and

750 Wisthaler, A.: The molecular identification of organic compounds in the atmosphere: state of the art and

751 challenges, *Chem. Rev.*, 115, 3919-3983, 10.1021/cr5003485, 2015.

752 Pereira, K. L., Hamilton, J. F., Rickard, A. R., Bloss, W. J., Alam, M. S., Camredon, M., Muñoz, A., Vázquez,

753 M., Borrás, E., and Ródenas, M.: Secondary organic aerosol formation and composition from the photo-

754 oxidation of methyl chavicol (estragole), *Atmos. Chem. Phys.*, 14, 5349-5368, 10.5194/acp-14-5349-

755 2014, 2014.

756 Perry, R. H., Cooks, R. G., and Noll, R. J.: ORBITRAP MASS SPECTROMETRY: INSTRUMENTATION,

757 ION MOTION AND APPLICATIONS, *Mass Spectrometry Reviews*, 27, 661-699, 10.1002/mas.20186,

758 2008.

759 Rincón, A. G., Calvo, A. I., Dietzel, M., and Kalberer, M.: Seasonal differences of urban organic aerosol

760 composition - an ultra-high resolution mass spectrometry study, *Environ. Chem.*, 9, 298,

761 10.1071/en12016, 2012.

762 Riva, M., Tomaz, S., Cui, T., Lin, Y.-H., Perraudin, E., Gold, A., Stone, E. A., Villenave, E., and Surratt, J.

763 D.: Evidence for an Unrecognized Secondary Anthropogenic Source of Organosulfates and Sulfonates:

764 Gas-Phase Oxidation of Polycyclic Aromatic Hydrocarbons in the Presence of Sulfate Aerosol, *Environ.*

765 *Sci. Technol.*, 49, 6654-6664, 10.1021/acs.est.5b00836, 2015.

766 Schmidt, A. C., Herzschuh, R., Matysik, F. M., and Engewald, W.: Investigation of the ionisation and

767 fragmentation behaviour of different nitroaromatic compounds occurring as polar metabolites of

768 explosives using electrospray ionisation tandem mass spectrometry, *Rapid Commun Mass Spectrom*, 20,

769 2293-2302, 10.1002/rcm.2591, 2006.

770 Shi, Z., Vu, T., Kotthaus, S., Harrison, R. M., Grimmond, S., Yue, S., Zhu, T., Lee, J., Han, Y., Demuzere,

771 M., Dunmore, R. E., Ren, L., Liu, D., Wang, Y., Wild, O., Allan, J., Acton, W. J., Barlow, J., Barratt, B.,

772 Beddows, D., Bloss, W. J., Calzolari, G., Carruthers, D., Carslaw, D. C., Chan, Q., Chatzidiakou, L., Chen,

773 Y., Crilley, L., Coe, H., Dai, T., Doherty, R., Duan, F., Fu, P., Ge, B., Ge, M., Guan, D., Hamilton, J. F.,

774 He, K., Heal, M., Heard, D., Hewitt, C. N., Hollaway, M., Hu, M., Ji, D., Jiang, X., Jones, R., Kalberer,

775 M., Kelly, F. J., Kramer, L., Langford, B., Lin, C., Lewis, A. C., Li, J., Li, W., Liu, H., Liu, J., Loh, M.,

776 Lu, K., Lucarelli, F., Mann, G., McFiggans, G., Miller, M. R., Mills, G., Monk, P., Nemitz, E., amp, apos,

777 Connor, F., Ouyang, B., Palmer, P. I., Percival, C., Popoola, O., Reeves, C., Rickard, A. R., Shao, L., Shi,

778 G., Spracklen, D., Stevenson, D., Sun, Y., Sun, Z., Tao, S., Tong, S., Wang, Q., Wang, W., Wang, X.,

779 Wang, X., Wang, Z., Wei, L., Whalley, L., Wu, X., Wu, Z., Xie, P., Yang, F., Zhang, Q., Zhang, Y.,

780 Zhang, Y., and Zheng, M.: Introduction to the special issue "In-depth study of air pollution sources and

781 processes within Beijing and its surrounding region (APHH-Beijing)", *Atmospheric Chemistry and*

782 *Physics*, 19, 7519-7546, 10.5194/acp-19-7519-2019, 2019.

783 Song, J., Li, M., Jiang, B., Wei, S., Fan, X., and Peng, P.: Molecular Characterization of Water-Soluble

784 Humic like Substances in Smoke Particles Emitted from Combustion of Biomass Materials and Coal

785 Using Ultrahigh-Resolution Electrospray Ionization Fourier Transform Ion Cyclotron Resonance Mass

786 Spectrometry, *Environ. Sci. Technol.*, 52, 2575-2585, 10.1021/acs.est.7b06126, 2018.
787 Sun, Y., Jiang, Q., Zhang, Z., Fu, P., Li, J., Yang, T., and Yin, Y.: Investigation of the sources and evolution
788 processes of severe haze pollution in Beijing in January 2013, *J. Geophys. Res.-Atmos.*, 119, 4380-4389,
789 10.1002/, 2014.
790 Surratt, J. D., Gomez-Gonzalez, Y., Chan, A. W., Vermeylen, R., Shahgholl, M., Kleindienst, T. E., Jaoui,
791 M., Maenhaut, W., Claeys, M., Flagan, R. C., and Seinfeld, J. H.: Evidence for Organosulfate in
792 Secondary Organic Aerosol, *Environ. Sci. Technol.*, 41, 517-527, 10.1021/es062081q, 2007.
793 Surratt, J. D., Gómez-González, Y., Chan, A. W., Vermeylen, R., Shahgholi, M., Kleindienst, T. E., Edney,
794 E. O., Offenberg, J. H., Lewandowski, M., Jaoui, M., Maenhaut, W., Claeys, M., Flagan, R. C., and
795 Seinfeld, J. H.: Organosulfate Formation in Biogenic Secondary Organic Aerosol, *J. Phys. Chem. A*, 112,
796 8345-8378, 2008.
797 Tao, S., Lu, X., Levac, N., Bateman, A. P., Nguyen, T. B., Bones, D. L., Nizkorodov, S. A., Laskin, J., Laskin,
798 A., and Yang, X.: Molecular Characterization of Organosulfates in Organic Aerosols from Shanghai and
799 Los Angeles Urban Areas by Nanospray-Desorption Electrospray Ionization High-Resolution Mass
800 Spectrometry, *Environ. Sci. Technol.*, 48, 10993-11001, 10.1021/es5024674, 2014.
801 Tong, H., Kourtchev, I., Pant, P., Keyte, I. J., O'Connor, I. P., Wenger, J. C., Pope, F. D., Harrison, R. M.,
802 and Kalberer, M.: Molecular composition of organic aerosols at urban background and road tunnel sites
803 using ultra-high resolution mass spectrometry, *Faraday Discuss.*, 189, 51-68, 10.1039/c5fd00206k, 2016.
804 Tong, H., Zhang, Y., Filippi, A., Wang, T., Li, C., Liu, F., Leppla, D., Kourtchev, I., Wang, K., Keskinen, H.
805 M., Levula, J. T., Arangio, A. M., Shen, F., Ditas, F., Martin, S. T., Artaxo, P., Godoi, R. H. M.,
806 Yamamoto, C. I., de Souza, R. A. F., Huang, R. J., Berkemeier, T., Wang, Y., Su, H., Cheng, Y., Pope,
807 F. D., Fu, P., Yao, M., Pohlker, C., Petaja, T., Kulmala, M., Andreae, M. O., Shiraiwa, M., Poschl, U.,
808 Hoffmann, T., and Kalberer, M.: Radical Formation by Fine Particulate Matter Associated with Highly
809 Oxygenated Molecules, *Environ Sci Technol*, 53, 12506-12518, 10.1021/acs.est.9b05149, 2019.
810 Tu, P., Hall, W. A. t., and Johnston, M. V.: Characterization of Highly Oxidized Molecules in Fresh and
811 Aged Biogenic Secondary Organic Aerosol, *Anal. Chem.*, 88, 4495-4501,
812 10.1021/acs.analchem.6b00378, 2016.
813 Wang, G., Kawamura, K., Umemoto, N., Xie, M., Hu, S., and Wang, Z.: Water-soluble organic compounds
814 in PM_{2.5} and size-segregated aerosols over Mount Tai in North China Plain, *J. Geophys. Res.*, 114,
815 10.1029/2008jd011390, 2009.
816 Wang, K., Zhang, Y., Huang, R.-J., Cao, J., and Hoffmann, T.: UHPLC-Orbitrap mass spectrometric
817 characterization of organic aerosol from a central European city (Mainz, Germany) and a Chinese
818 megacity (Beijing), *Atmos. Environ.*, 189, 22-29, 10.1016/j.atmosenv.2018.06.036, 2018.
819 Wang, K., Zhang, Y., Huang, R.-J., Wang, M., Ni, H., Kampf, C. J., Cheng, Y., Bilde, M., Glasius, M., and
820 Hoffmann, T.: Molecular characterization and source identification of atmospheric particulate
821 organosulfates using ultrahigh resolution mass spectrometry, *Environ. Sci. Technol.*,
822 10.1021/acs.est.9b02628, 2019a.
823 Wang, M., Huang, R.-J., Cao, J., Dai, W., Zhou, J., Lin, C., Ni, H., Duan, J., Wang, T., Chen, Y., Li, Y.,
824 Chen, Q., Haddad, I. E., and Hoffmann, T.: Determination of n-alkanes, PAHs and hopanes in
825 atmospheric aerosol: evaluation and comparison of thermal desorption GC-MS and solvent extraction
826 GC-MS approaches, *Atmos. Mea. Tech. Discuss.*, 1-21, 10.5194/amt-2019-4, 2019b.
827 Wang, X. K., Rossignol, S., Ma, Y., Yao, L., Wang, M. Y., Chen, J. M., George, C., and Wang, L.: Molecular
828 characterization of atmospheric particulate organosulfates in three megacities at the middle and lower
829 reaches of the Yangtze River, *Atmos. Chem. Phys.*, 16, 2285-2298, [https://doi.org/10.5194/acp-16-2285-](https://doi.org/10.5194/acp-16-2285-2016)
830 [2016](https://doi.org/10.5194/acp-16-2285-2016), 2016.
831 Wang, X. K., Hayeck, N., Brüggemann, M., Yao, L., Chen, H. F., Zhang, C., Emmelin, C., Chen, J. M.,
832 George, C., and Wang, L.: Chemical characterization of organic aerosol in: A study by Ultrahigh-
833 Performance Liquid Chromatography Coupled with Orbitrap Mass Spectrometry, *J. Geophys. Res.-Atmos.*,
834 122, 703-722, <https://doi.org/10.1002/2017JD026930>, 2017.
835 Xu, W., Sun, Y., Wang, Q., Zhao, J., Wang, J., Ge, X., Xie, C., Zhou, W., Du, W., Li, J., Fu, P., Wang, Z.,
836 Worsnop, D. R., and Coe, H.: Changes in Aerosol Chemistry From 2014 to 2016 in Winter in Beijing:
837 Insights From High-Resolution Aerosol Mass Spectrometry, *J. Geophys. Res.-Atmos.*, 124, 1132-1147,
838 10.1029/2018jd029245, 2019.
839 Yassine, M. M., Harir, M., Dabek-Zlotorzynska, E., and Schmitt-Kopplin, P.: Structural characterization of
840 organic aerosol using Fourier transform ion cyclotron resonance mass spectrometry: aromaticity

841 equivalent approach, *Rapid Commun. Mass Spectrom.*, 28, 2445-2454, 10.1002/rcm.7038, 2014.
842 Zhang, P.: Revitalizing old industrial base of Northeast China: Process, policy and challenge, *Chin. Geogra.*
843 *Sci.*, 18, 109-118, 10.1007/s11769-008-0109-2, 2008.
844 Zielinski, A. T., Kourtchev, I., Bortolini, C., Fuller, S. J., Giorio, C., Popoola, O. A. M., Bogialli, S., Tapparo,
845 A., Jones, R. L., and Kalberer, M.: A new processing scheme for ultra-high resolution direct infusion
846 mass spectrometry data, *Atmos. Environ.*, 178, 129-139, 10.1016/j.atmosenv.2018.01.034, 2018.

847

848

849

850

851

852

853

854

855

856

857

858

859

860

861

862

863

864

865

866

867

868

869

870

871

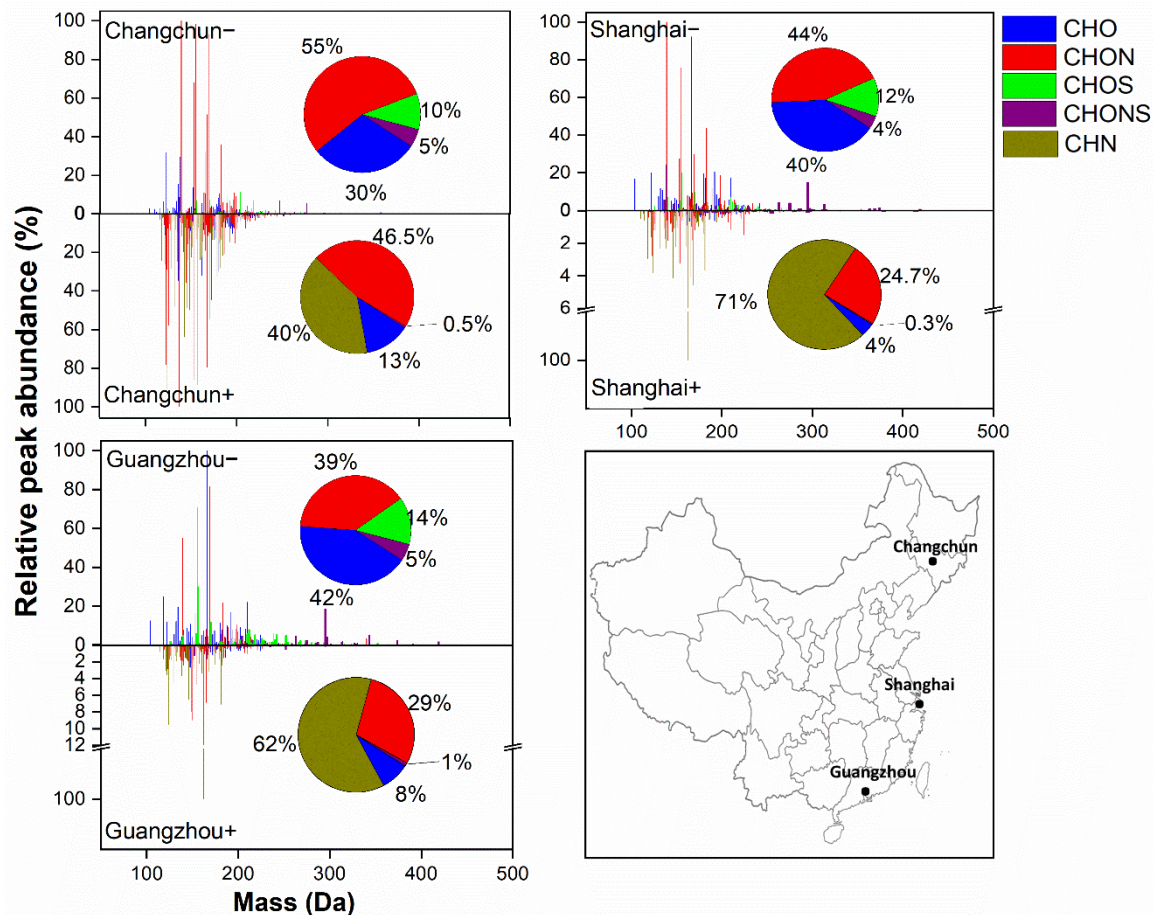
872

873 Table 1. Number of organic compounds and molecular formulas in each subgroup and the peak
 874 abundance-weighted average values of molecular mass (MM_{avg}), elemental ratios, double bond
 875 equivalent (DBE), aromaticity equivalent (X_c) and isomer number fraction (meaning the
 876 percentage of formula numbers that have isomers among all assigned formulas) for detected
 877 organic compounds in ESI⁻ and ESI⁺ in the three Chinese cities.

Sample ID	Subgroup	Number of compounds*	Relative abundance (%)	MM_{avg}	H/C	O/C**	DBE	X_c	Isomer number fraction (%)
Changchun ⁻	total	769(415)	100	169	1.03	0.58	5.02	2.13	34
	CHO ⁻	346(136)	30	162	0.96	0.41	5.65	2.28	52
	CHON ⁻	180(96)	55	163	0.94	0.51	5.24	2.44	36
	CHOS ⁻	155(105)	10	198	1.56	1.17(0.52)	2.55	0.50	28
	CHONS ⁻	88(78)	5	214	1.35	1.07(-1.4)	3.75	1.06	8
Shanghai ⁻	total	416(272)	100	176	1.05	0.69	4.99	1.92	31
	CHO ⁻	164(90)	40	171	0.97	0.59	5.37	1.94	41
	CHON ⁻	135(89)	44	169	0.86	0.56	5.67	2.47	37
	CHOS ⁻	75(62)	12	190	1.85	1.41(0.61)	1.79	0.34	15
	CHONS ⁻	42(31)	4	266	1.56	1.00(0.11)	3.30	0.44	13
Guangzhou ⁻	total	488(304)	100	183	1.14	0.74	4.55	1.65	34
	CHO ⁻	196(110)	42	172	1.10	0.65	4.68	1.57	44
	CHON ⁻	161(98)	39	173	0.89	0.58	5.56	2.41	35
	CHOS ⁻	86(67)	14	201	1.85	1.48(0.71)	1.71	0.21	21
	CHONS ⁻	45(29)	5	293	1.56	0.82(0.06)	3.45	0.43	28
Changchun ⁺	total	2943(679)	100	160	1.21	0.13	5.58	2.36	56
	CHO ⁺	609(162)	13	174	0.94	0.28	6.55	2.22	50
	CHN ⁺	696(126)	40	154	1.22	0.00	5.84	2.60	77
	CHON ⁺	1594(352)	46.5	161	1.27	0.19	5.11	2.22	55
	CHONS ⁺	44(39)	0.5	196	1.91	0.70	2.64	0.09	13
Shanghai ⁺	total	704(383)	100	162	1.37	0.09	4.91	2.32	32
	CHO ⁺	87(67)	4	184	1.13	0.43	5.46	1.46	19
	CHN ⁺	253(84)	71	159	1.38	0.00	5.08	2.55	54
	CHON ⁺	350(218)	24.7	167	1.40	0.27	4.34	1.81	30
	CHONS ⁺	14(14)	0.3	241	1.17	0.61	5.32	0.91	0
Guangzhou ⁺	total	687(412)	100	161	1.41	0.17	4.58	2.07	30
	CHO ⁺	125(87)	8	185	1.12	0.42	5.19	1.20	26
	CHN ⁺	205(78)	62	156	1.42	0.00	4.80	2.47	54
	CHON ⁺	336(227)	29	165	1.47	0.45	4.00	1.51	26
	CHONS ⁺	21(20)	1	209	1.84	0.71	3.05	0.31	5

878 *The values in brackets indicate the number of unique molecular formulas. **The values in brackets indicate the
 879 (O-3S)/C and (O-3S-2N)/C ratios for CHOS and CHONS compounds, respectively, detected in ESI⁻ mode

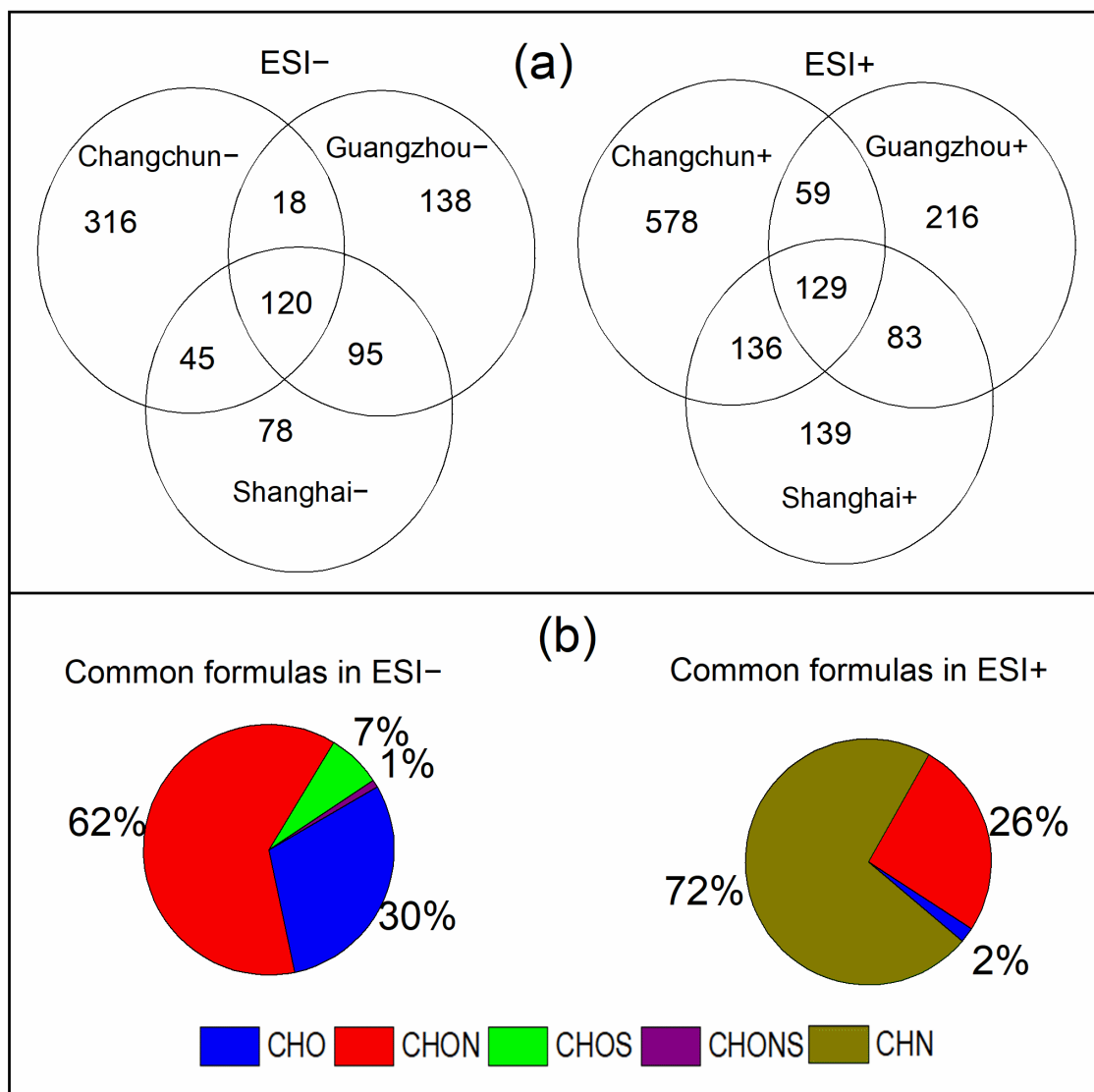
880



881

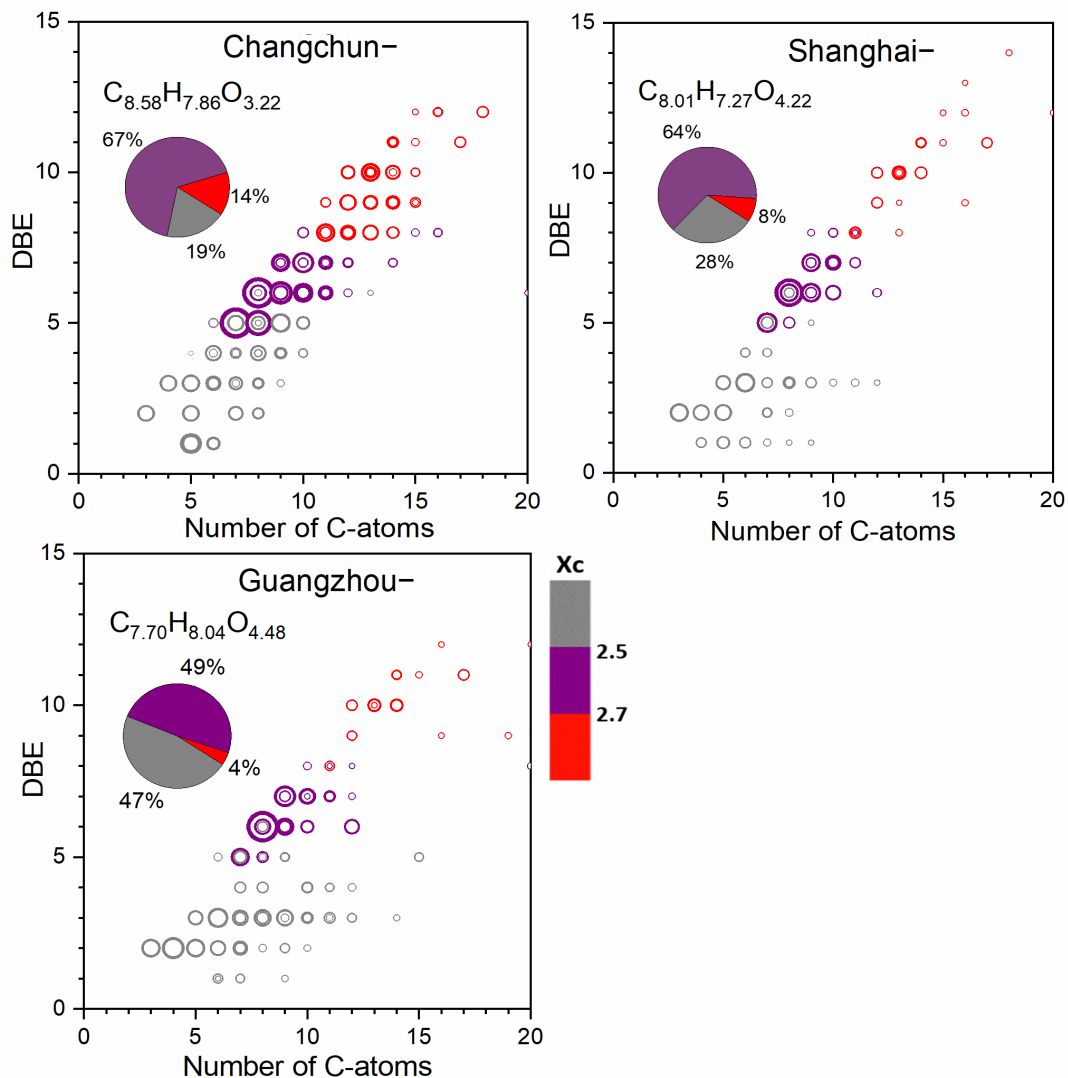
882 Figure 1. Mass spectra of detected organic compounds reconstructed from extracted ion
 883 chromatograms in ESI⁻ and ESI⁺. The horizontal axis refers to the molecular mass (Da) of the
 884 identified species. The vertical axis refers to the relative peak abundance of each individual
 885 compound to the compound with the greatest peak abundance. The pie charts show the percentage
 886 of each organic compound subgroup (i.e. CHO, CHON, CHOS, CHONS and CHN) in each sample
 887 in terms of peak abundance. The map in the lower right corner shows the locations of these three
 888 megacities in China.

889



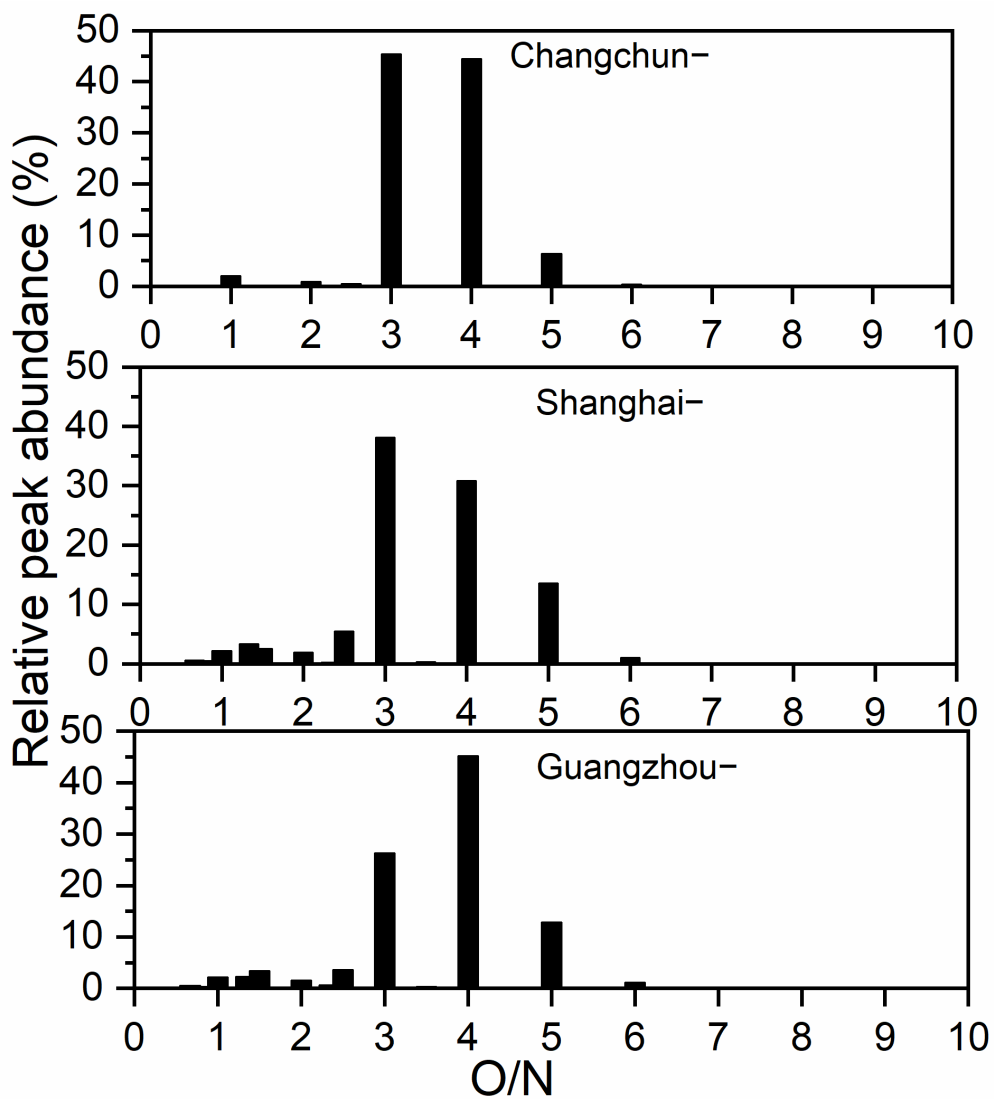
890

891 Figure 2. (a) Venn diagrams showing the number distribution of all molecular formulas detected in
 892 ESI⁻ and ESI⁺ for all sample locations. The overlapping molecular formulas refer to the
 893 compounds detected in each city with the same molecular formulas and with the same retention
 894 times (retention time difference ≤ 0.1 min). (b) Peak abundance contribution of each elemental
 895 formula category to the total common formulas.



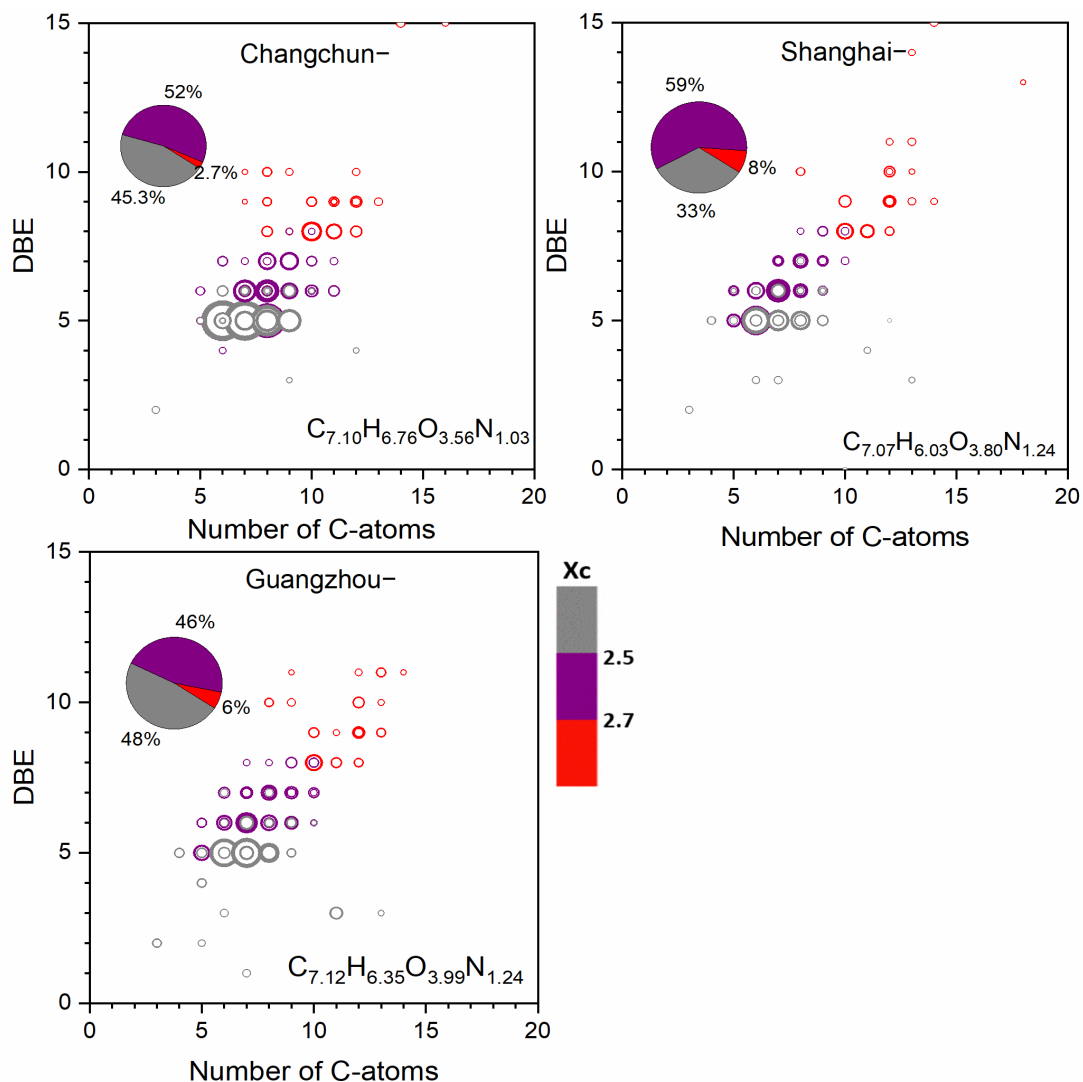
896

897 Figure 3. Double bond equivalent (DBE) versus carbon number for all CHO- compounds for all
 898 sample locations. The molecular formula represents the abundance-weighted average CHO-
 899 formula and the area of the circles is proportional to the fourth root of the peak abundance of an
 900 individual compound (a diagram with circle areas related to the absolute peak abundances is
 901 presented in Fig. S2). The color bar denotes the aromaticity equivalent (gray with $X_c < 2.50$, purple
 902 with $2.50 \leq X_c < 2.70$ and red with $X_c \geq 2.70$). The pie charts show the percentage of each X_c
 903 category (i.e., gray color-coded compounds, purple color-coded compounds and red color-coded
 904 compounds) in each sample in terms of peak abundance.



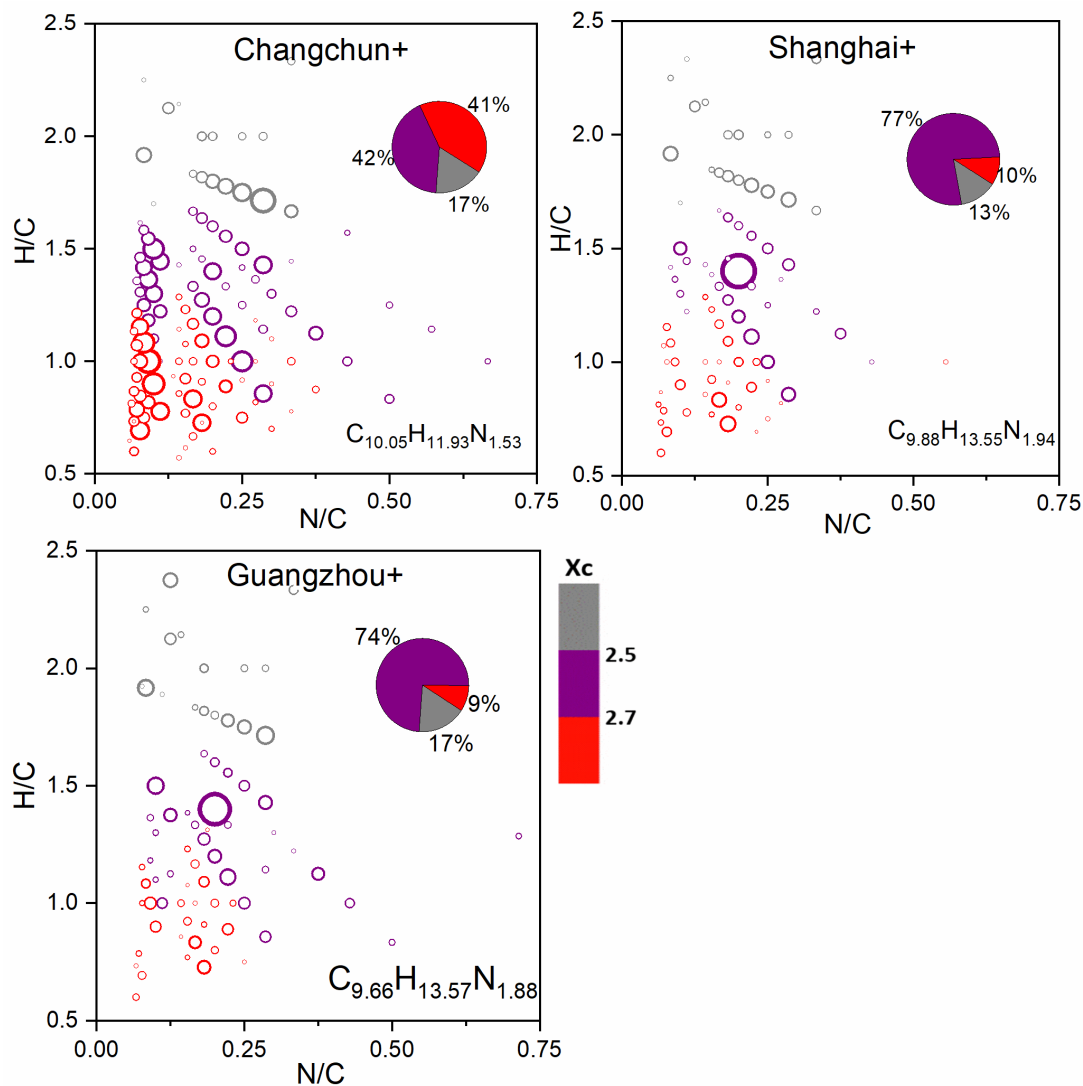
905

906 Figure 4. Classification of CHON⁻ compounds into different subgroups according to O/N ratios in
 907 their formulas. The y-axis indicates the relative contribution of each specific O/N ratio subgroup to
 908 the sum of peak abundances of CHON⁻ compounds.



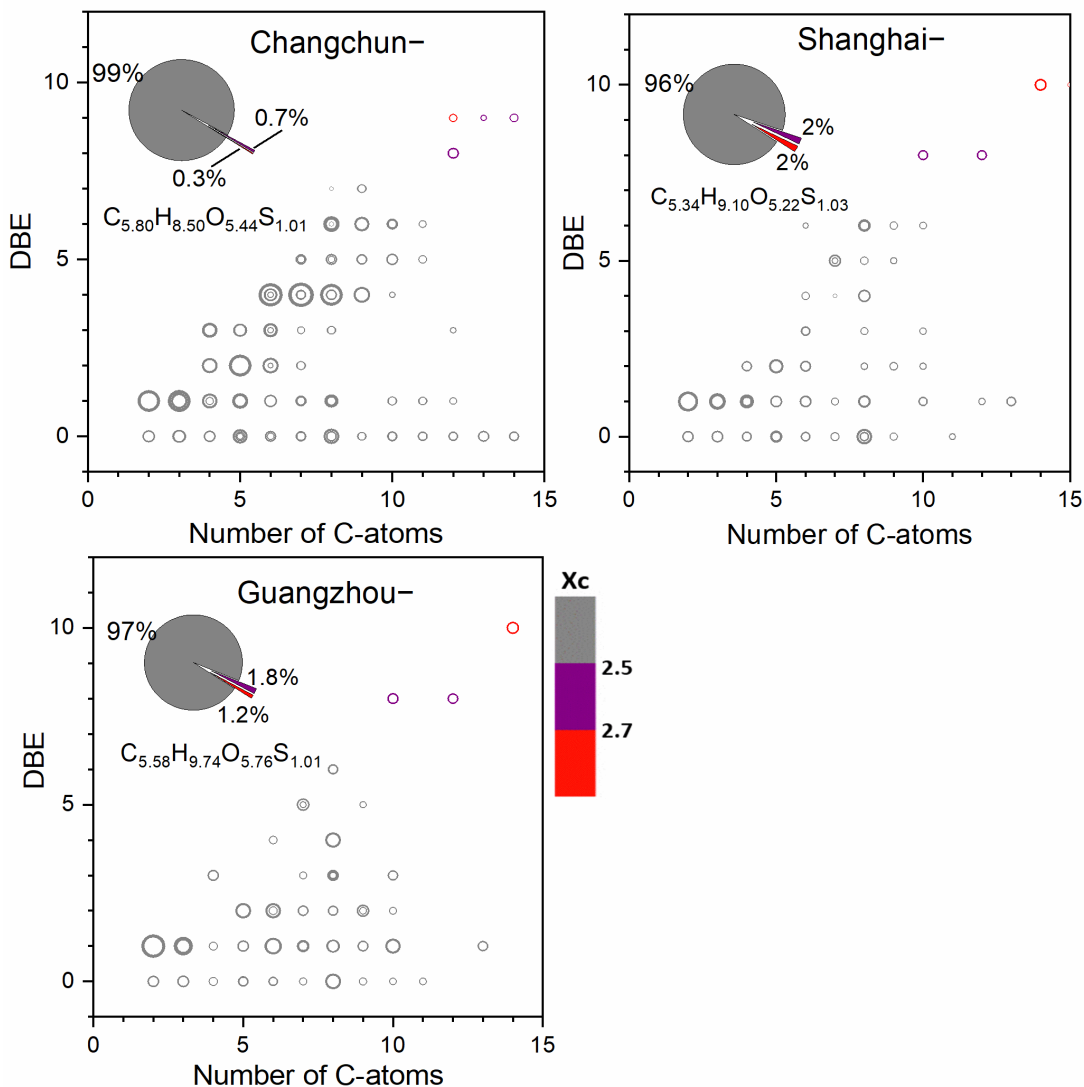
909

910 Figure 5. Double bond equivalent (DBE) versus carbon number for all CHON⁻ compounds for all
 911 sample locations. The molecular formula represents the abundance-weighted average CHON-
 912 formula and the area of circles is proportional to the fourth root of the peak abundance of an
 913 individual compound (a diagram with circle areas related to absolute peak abundances is presented
 914 in Fig. S6). The color bar denotes the aromaticity equivalent (gray with X_c < 2.50, purple with 2.50
 915 ≤ X_c < 2.70 and red with X_c ≥ 2.70). The pie charts show the percentage of each X_c category (i.e.,
 916 gray color-coded compounds, purple color-coded compounds and red color-coded compounds) in
 917 each sample in terms of peak abundance.



918

919 Figure 6. Van Krevelen diagrams for CHN+ compounds in Changchun, Shanghai and Guangzhou
 920 samples. The area of circles is proportional to the fourth root of the peak abundance of an individual
 921 compound (a diagram with circle areas related to absolute peak abundances is presented in Fig.
 922 S10) and the color bar denotes the aromaticity equivalent (gray with $X_c < 2.50$, purple with $2.50 \leq$
 923 $X_c < 2.70$ and red with $X_c \geq 2.70$). The pie charts show the percentage of each X_c category (i.e.,
 924 gray color-coded compounds, purple color-coded compounds and red color-coded compounds) in
 925 each sample in terms of peak abundance.



926

927 Figure 7. Double bond equivalent (DBE) versus carbon number for all CHOS- compounds for all
 928 sample locations. The molecular formula represents the abundance-weighted average CHOS-
 929 formula and the area of circles is proportional to the fourth root of the peak abundance of an
 930 individual compound (a diagram with circle areas related to absolute peak abundances is presented
 931 in Fig. S11). The color bar denotes the aromaticity equivalent (gray with $X_c < 2.50$, purple with
 932 $2.50 \leq X_c < 2.70$ and red with $X_c \geq 2.70$). The pie charts show the percentage of each X_c category
 933 (i.e., gray color-coded compounds, purple color-coded compounds and red color-coded compounds)
 934 in each sample in terms of peak abundance.

935

936

937